



Australian Government
Department of Defence
Defence Science and
Technology Organisation

A Crack Growth Rate Conversion Module: Theory, Development, User Guide and Examples

Yu Chee Tong, Weiping Hu and David Mongru

Air Vehicles Division
Defence Science and Technology Organisation

DSTO-TR-2050

ABSTRACT

The use of crack growth analysis tools based on plasticity-induced crack closure model, such as FASTRAN, CGAP and AFGROW, requires the conversion of crack growth rate versus the nominal stress intensity range curves to a "single" curve of crack growth rate versus the effective stress intensity range. In order to minimise the error arising from crack growth rate conversion and judiciously utilise these software tools, a user-friendly tool was integrated into CGAP. This report documents the theory, implementation, the user guide and examples of the crack growth rate conversion software module.

RELEASE LIMITATION

Approved for public release

Published by

*Air Vehicles Division
DSTO Defence Science and Technology Organisation
506 Lorimer St
Fishermans Bend, Victoria 3207 Australia*

*Telephone: (03) 9626 7000
Fax: (03) 9626 7999*

*© Commonwealth of Australia 2007
AR-014-020
September 2007*

APPROVED FOR PUBLIC RELEASE

A Crack Growth Rate Conversion Module: Theory, Development, User Guide and Examples

Executive Summary

Crack growth assessment is an essential element of the aircraft certification procedure for addressing structural durability and fatigue concerns on all Australian Defence Force (ADF) air platforms.

The current modelling tools for fatigue crack growth all involve numerous assumptions and extrapolation methodologies, in order to estimate the life of a real structure from the data obtained from simple coupon tests. These assumptions introduce uncertainties not only in the results themselves but also in the procedures used to obtain the results. There is, therefore, a need for DSTO to explicitly define the procedures in each stage of crack growth analyses, including data conversion.

As an example of the efforts to codify the knowledge in this area, this report develops and documents procedures for the intuitive and routine processing of crack growth rate data, in order to allow fatigue life prediction tools to be applied appropriately, and any correlation and comparison with experimental data to be made rigorously. The use of crack growth assessment tools based on the plasticity-induced crack closure model, such as FASTRAN, CGAP and AFGROW, requires a single curve of crack growth rate versus effective stress intensity range, where the effective stress intensity range is dependent on the crack opening stress. However, the available experimental growth rates are routinely defined against the nominal stress intensity range, with the stress ratio as a parameter. Therefore, the crack growth rate versus the nominal stress intensity range needs to be converted to a "single" curve of growth rate versus the effective stress intensity range. This conversion is by no means straightforward. In order to minimise the error arising from the conversion and judicious use of software, a user-friendly tool for conversion of crack growth rate has been developed, implemented and integrated into CGAP.

This report presents the theory and the algorithms involved in the conversion methodology. It discusses, in detail, the concept of plasticity-induced crack closure, crack opening stress, the constraint factor and the plasticity-corrected stress intensity factor. A user manual and examples are included to assist the use of this software module in CGAP.

Authors

Yu Chee Tong Air Vehicles Division

Dr Chee Tong is presently a research scientist in the Air Vehicles division of DSTO. He joined AVD-DSTO in 1999 after graduating from the Royal Melbourne Institute of Technology with a Bachelor Degree in Aerospace Engineering with Honours. In 2006, he completed his Ph.D. at the University of Sydney, supported by AVD-DSTO, on probabilistic fatigue life analysis methods for aerospace vehicles. Since joining DSTO in 1999, Dr Tong has worked in the fields of structural risk and reliability for airframe, engine and helicopter components, propulsion systems life management, fracture mechanics research, aircraft structural lifing standards, and structural lifing methodologies and tools. Currently, he is working in the areas air vehicle risk and reliability assessment, and structural lifing methodologies and tools.

Weiping Hu Air Vehicles Division

Dr Weiping Hu joined DSTO in 1998 as a research scientist. He is currently a senior research scientist leading the development of modelling capabilities for the analysis of structural integrity of aircraft structures.

After obtaining his PhD degree in 1993 at Dublin City Univeristy, Ireland, he held various academic positions at Dublin City University, Monash University and Deakin University. His research interests include fatigue and fracture of engineering materials and structures, fatigue crack growth in aircraft structures, constitutive models and plasticity, and numerical methods in engineering.

David Mongru
Air Vehicles Division

Mr Mongru graduated from RMIT in 1990 with a Bachelor of Aerospace Engineering (Honours). He commenced work at DSTO in 1994 working on loads development and fatigue interpretation for the PC9 fatigue test. He joined IFOSTP in 1996 performing fatigue analysis of critical components on the aft fuselage of the F/A-18. In 2001 he commenced work on the P-3 SLAP. His primary functions included fatigue test interpretation and provision of technical support to the P-3 empennage test. He is currently working on the standards and lifing methodologies task.

Contents

1. INTRODUCTION	1
2. FUNDAMENTALS OF FATIGUE CRACK GROWTH MODELLING	2
2.1 Linear Elastic Fracture Mechanics and Paris Law	2
2.2 Mechanical Loading Effects	4
2.2.1 Stress Ratio Effect	4
2.2.2 Load Interaction Effect	5
2.3 Plasticity-Induced Crack Closure	5
2.4 Fatigue Crack Growth Rate Modelling	7
2.5 Elastic-Plastic Effective Stress Intensity Factors	8
3. NEWMAN'S CRACK OPENING STRESS EQUATIONS	9
3.1 Centre-Crack Tension (CCT) Specimen	10
3.2 Compact Tension (CT) Specimen	11
3.3 Limitations	12
4. DKEFF PROGRAM AND CGAP CRACK GROWTH RATE CONVERSION MODULE	14
4.1 Effective Stress Intensity Factor Calculation	15
4.2 Constant Constraint Factor	15
4.3 Variable Constraint Factor	16
5. EXAMPLES	18
5.1 7050-T7451 Aluminium Alloy Example	18
5.1.1 Constant Constraint Factor	19
5.1.2 Variable Constraint Factors	22
5.2 2219-T851 Aluminium Alloy Example	23
5.2.1 Constant Constraint Factor	25
5.2.2 Variable Constraint Factor	25
6. DISCUSSION	26
6.1 Finding the Optimum Constraint Factor	26
6.2 Limitations	26
7. SUMMARY AND FUTURE WORK	27
REFERENCE	28
APPENDIX A - CGAP CRACK GROWTH RATE CONVERTER: USER GUIDE	31
A.1. Introduction	31
A.2. FCGR Program Flowchart	31
A.3. Running FCGR	31

A.4. Example Problem Using 7075-T651.....	44
APPENDIX B - COEFFICIENT OF DETERMINATION	47
APPENDIX C INPUT FILES FOR THE EXAMPLES	49

Nomenclature

a	Crack length, or half length for a symmetric crack.
C	Crack growth rate coefficient in Paris law.
C_5	Cyclic fracture toughness.
F	Geometry correction factor.
G	Threshold function, $G = 1 - (\Delta K_0 / \Delta K_{\text{eff}})^p$.
H	Fracture function, $H = 1 - (K_{\text{max}} / C_5)^q$.
m	Crack growth rate exponent in Paris law.
N	Number of cycles.
K	Stress intensity factor.
K_C	Fracture toughness.
K_{max}	Maximum stress intensity factor.
ΔK	Stress intensity factor range.
ΔK_0	Long crack threshold. It is considered to be a material constant, and in particular, independent of crack length.
ΔK_{eff}	Effective stress intensity range.
P	Load.
R	Stress ratio of a load cycle, $R_S = S_{\text{min}} / S_{\text{max}}$.
S	Applied remote stress.
ΔS_{eff}	Effective stress range, $\Delta S_{\text{eff}} = S_{\text{max}} - S_o$
S_{max}	The maximum stress in a load cycle.
S_{min}	The minimum stress in a load cycle.
S_o	Crack opening stress.
ΔS	Applied stress range. $\Delta S = S_{\text{max}} - S_{\text{min}}$.
t	Thickness of the specimen.
U	Effective stress intensity factor ratio, $U = \frac{\Delta K_{\text{eff}}}{\Delta K} = \frac{S_{\text{max}} - S_o}{S_{\text{max}} - S_{\text{min}}} = \frac{1 - \gamma}{1 - R}$
W	Specimen width, or half width for symmetric crack.
γ	$\gamma = S_o / S_{\text{max}}$
λ	$\lambda = a / W$.
ρ	Plastic zone size.
σ	Local stress.
σ_0	Averaged flow stress, $\sigma_0 = (\sigma_y + \sigma_u) / 2$.
$\Delta \sigma_e$	Endurance limit.
σ_{max}	Local maximum stress.
σ_{min}	Local minimum stress.
σ_u	Ultimate stress of material.
σ_y	Uniaxial yield stress of material.
ω	Cyclic plastic zone size.

1. Introduction

Crack growth assessment is an essential element of the aircraft certification procedure for addressing structural durability and fatigue concerns of all Australian Defence Force (ADF) air platforms. It provides a means for estimating and assessing the growth of fatigue cracks in structures from flaws either pre-existing at the time of manufacture or generated under in-service conditions. The output of the assessment provides guidance for the development of inspection programs to ensure the timely detection of fatigue cracks in components or to allow repair or replacement of the components, wherever feasible, to be carried out.

The current modelling methodologies for fatigue crack growth are, to varying degrees, empirical in nature. In classical linear elastic fracture mechanics (LEFM), the quantitative prediction of fatigue crack growth in structures is obtained by extrapolating the characteristic fatigue crack growth rate (FCGR) data derived from simple crack growth tests using an appropriate crack growth model. As a result, the accuracy of fatigue crack growth life prediction can be significantly affected by the uncertainty in the source data and the uncertainty in the procedures used to process the data. For the judicious use of crack growth analysis tools, it is highly desirable to codify the procedures for data processing, to ensure that the data are processed consistently, and any correlation and comparison of analytical results with experimental data be made meaningfully and rigorously.

The plasticity-induced crack closure model has been one of the most widely used models for characterising FCGR under constant amplitude loading and predicting fatigue crack growth under variable amplitude loading in recent decades. Some of the computer programs used in DSTO for crack growth analysis are fully or partially based on this model, such as FASTRAN [1], AFGROW¹ [2] and CGAP [3]. These programs require the FCGR da/dN be defined by a "single" curve against the effective stress intensity factor (SIF) range ΔK_{eff} , but FCGR data are traditionally plotted against the nominal SIF range ΔK for different stress ratios R . Due to the complexity in the calculation of the crack opening stress, the conversion to a single da/dN versus ΔK_{eff} relation is neither simple nor straightforward. Therefore, it has been recognised [4] that there is an immediate need to develop a user-friendly tool to codify this conversion procedure, in order to minimise the uncertainties arising from this FCGR conversion process, and better utilise these software tools.

This report details the principle and the implementation of the FCGR conversion procedure. The FCGR conversion module, based on Newman's work [1], has been integrated into CGAP to take advantage of its graphical user interface. This FCGR conversion module enables the conversion of the nominal FCGR data to a da/dN versus

¹ Crack closure is one of the options available.

ΔK_{eff} curve, allowing the rate generation and fatigue crack growth analysis to be carried out within a single software environment. This report discusses the concept of crack closure, the relationship between the nominal SIF and the effective SIF, the determination of crack opening stress, and the procedures involved in the FCGR conversion. It also documents the FCGR conversion module under the CGAP graphical user interface. Some examples are also included to demonstrate the use of this software within the CGAP environment.

2. Fundamentals of Fatigue Crack Growth Modelling

This section provides a brief introduction to the crack growth models used by FASTRAN, CGAP and AFGROW.

2.1 Linear Elastic Fracture Mechanics and Paris Law

In 1957, Irwin [5] derived the linear elastic stress solutions for an isolated flaw inside an infinite plate that formed the foundation of linear elastic fracture mechanics (LEFM). Irwin identified three basic modes [6, 7] of fracture, (I) the opening mode, (II) the shear mode and (III) the anti-plane shear mode, and subsequently derived the linear elastic solutions of stresses and displacements for these three modes of fracture. As an example, for the opening mode (mode-I) with an isolated flaw of length $2a$ subjected to a uniform far-field stress S inside an infinite plate, as shown in Figure 1, the stress components are given as,

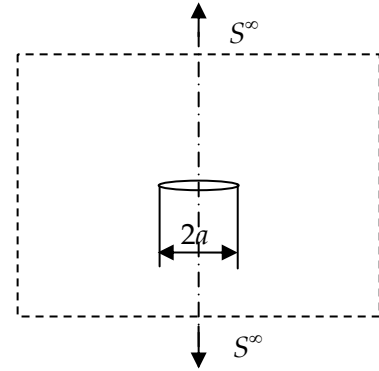


Figure 1 A central mode I crack in an infinite plate subjected to uniform far-field stress

$$\begin{bmatrix} S_{xx} \\ S_{yy} \\ \tau_{xy} \end{bmatrix} = \frac{K_I}{\sqrt{2\pi r}} \begin{bmatrix} \cos \frac{\theta}{2} \left(1 - \sin \frac{\theta}{2} \sin \frac{3\theta}{2} \right) \\ \cos \frac{\theta}{2} \left(1 + \sin \frac{\theta}{2} \sin \frac{3\theta}{2} \right) \\ \cos \frac{\theta}{2} \sin \frac{\theta}{2} \cos \frac{3\theta}{2} \end{bmatrix} + \dots \quad (1)$$

where r is the distance from the crack tip, and θ is the angle between the crack plane and r .

The parameter K in these stress equations has been termed the SIF, and the subscript I is used to indicate the mode-I fracture. Similar solutions of stresses for the other modes of fracture were also derived, with K_{II} and K_{III} , respectively, replacing K_I in the above equation. Depending on the load and geometry, all three modes of crack opening or

fracture may co-exist during crack extension, but under uniaxial loading and when the crack is long, the tensile opening mode K_I is dominant.

The significant outcome from Irwin's stress equations is that it shows the stress field inside a linear elastic body containing an isolated flaw and subjected to a far field applied stress is uniquely characterized by a single parameter, K . This means that provided K for any combination of crack length, geometry and applied stress is the same, the stress, strain and deformation would also be the same. This principle, known as *the principle of similitude*, is applicable in the slow stable growth stage. The significance of the principle is that it provides a theoretical basis for allowing the material response of simple laboratory specimens to be extrapolated to that of real engineering structures, and vice versa.

However, the principle of similitude breaks down in the short crack regime [8] where the crack length is either comparable to the size of the microstructures, or it is comparable to the crack tip plastic zone size. Furthermore, these linear elastic stress solutions predict an infinite stress at the crack tip ($r=0$) (meaning a sharp crack has a stress concentration factor of infinity), a situation that cannot exist in real materials. This anomaly implies that a region of plastically-deformed material may exist at the crack tip. This plastically-deformed region in the vicinity of the crack tip has a significant influence on the FCGR.

Under cyclic fatigue loading, Paris et al [9] related the FCGR, da/dN , to the SIF range, ΔK , to give

$$\frac{da}{dN} = C\Delta K^m. \quad (2)$$

This is now well-known as the Paris law. Here C and m are regression parameters but are also known as the FCGR coefficient and exponent, respectively. This empirical relationship was based on the principle of similitude and experimental evidence obtained for long cracks and constant amplitude testing. An example of this is shown in Figure 2. It is customary to obtain such long crack da/dN versus ΔK data for a material from constant amplitude loading crack growth tests on either compact tension (CT) or centre-crack tension (CCT) specimens.

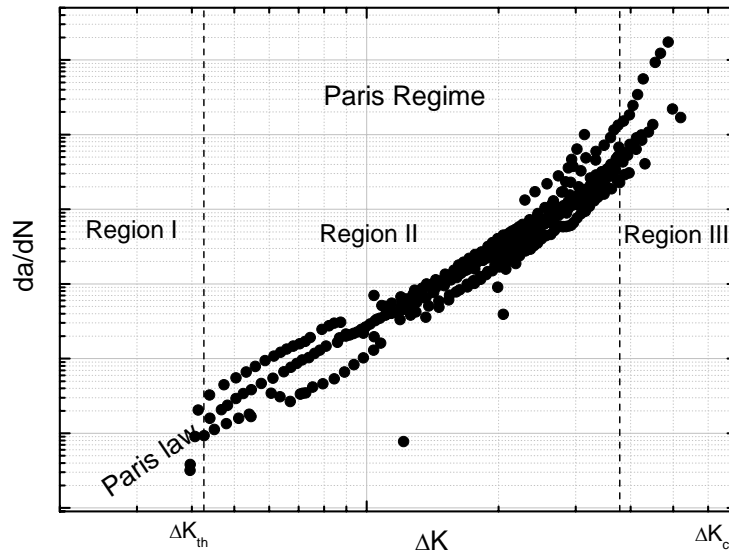


Figure 2: FCGR behaviour for long crack under constant amplitude loading

As shown in Figure 2, the Paris law only applies in region II or the *Paris regime*. Graphically the parameters C and m are simply the parameters of linear regression of da/dN versus ΔK data within this region plotted on a double logarithm scale. Region I shows that there is a stress intensity range threshold, ΔK_0 , below which long cracks will not grow. Region III, right of the Paris regime, shows increasingly higher FCGR, signalling the final fracture of the component as K_{\max} approaches K_C , the fracture toughness of the material. Note that at $K_{\max} = K_C$, $\Delta K_C = K_C(1 - R)$, since the effect of crack closure is not relevant at this point of loading. Then, for long cracks the fatigue crack propagation life, N_p , can be obtained by numerically summing Equation (2) cycle by cycle from the initial crack length until the critical SIF is reached, or until any other failure criterion is met, such as gross section yield.

2.2 Mechanical Loading Effects

The rate of fatigue crack growth is influenced by various mechanical loading and environmental effects, which are not taken into account by the Paris law. Numerous modifications and corrections have been made to the Paris law, in an attempt to better characterise fatigue crack growth behaviour. In this investigation however, only mechanical loading effects, in particular the effects of stress ratio and load sequence, at room temperature are considered.

2.2.1 Stress Ratio Effect

Under the same cyclic SIF range, FCGRs vary with the stress ratio, $R = S_{\min}/S_{\max}$. Figure 3 shows the effect of stress ratio on FCGR for the 7050-T7451 aluminium alloy. These data

were obtained from Sharp et al [10]. The effect of R -ratio on FCGR is not surprising because a change in the R -ratio for the same ΔK means a change in the mean stress, which in turn, affects the plastic deformation at the crack tip. The obvious explanation for the R -ratio effect on FCGR is that the cyclic plastic deformation (or fatigue damage) at the crack tip is a function of maximum and minimum SIFs. In general, an increase in the R -ratio means an increase in the mean or maximum and minimum applied stress, which results in faster crack growth, as demonstrated in Figure 3.

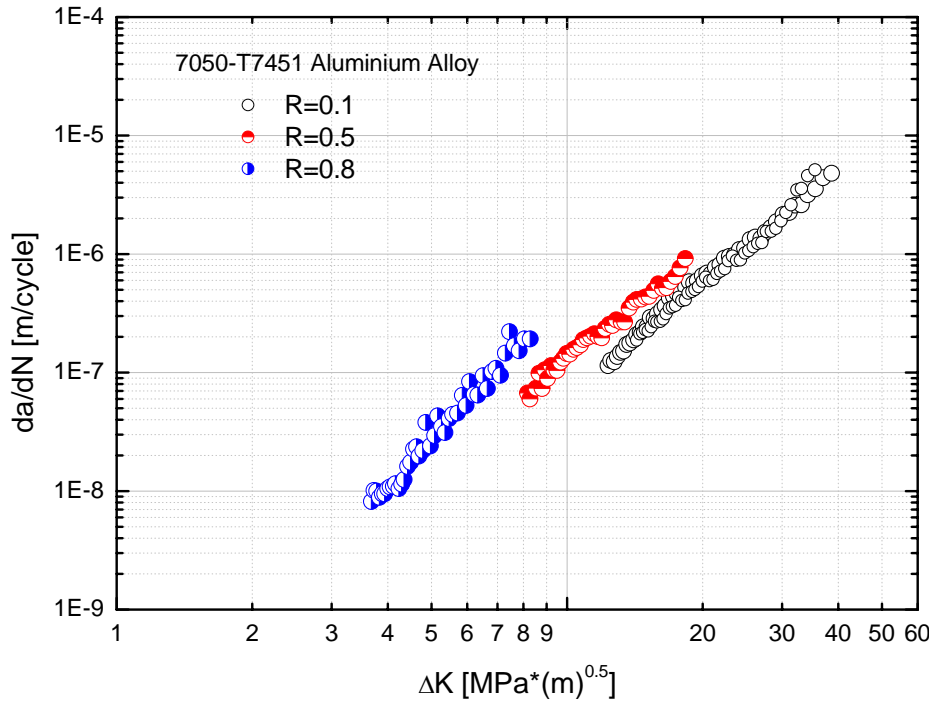


Figure 3: The effect of R -ratio on FCGR for 7050-T7451 aluminium alloy

2.2.2 Load Interaction Effect

Another important mechanical loading effect for fatigue crack growth modelling is the load interaction effect. Load interaction effects consist of retardation and acceleration observed in FCGR following overloads and underloads, respectively. These retardation and acceleration behaviours imply that the sequence of loading within a variable amplitude load spectrum can significantly affect the FCGRs and hence, alter the crack growth behaviour of the structure. It is, therefore, paramount that the FCGR prediction model can account for the loading interaction effect for reliable crack growth assessment.

2.3 Plasticity-Induced Crack Closure

The phenomenon of plasticity-induced crack closure [11, 12] is one of the most widely accepted mechanisms for explaining mechanical loading effects. The effective SIF concept [11] is widely utilised in recent times for making analytical fatigue crack growth life predictions. Details of this concept are presented in this section.

Elber [11] in 1970 observed that crack surfaces remain closed during part of the cycle under tension-tension cyclic loading, and subsequently suggested that this behaviour was attributed to the residual plastic deformation left in the wake of the advancing crack tip, causing the crack surfaces to be in contact before the remote load reaches zero. Based on this observation, Elber proposed that crack extension only occurs when the crack is open, so instead of using the full stress range intensity factor (SIF) range, ΔK , as a crack driving force, the range of SIF for which the crack is fully open should be used. This SIF range is known as the effective SIF, ΔK_{eff} , and is defined as,

$$\Delta K_{\text{eff}} = \beta(a) \Delta S_{\text{eff}} \sqrt{\pi a} \quad (3)$$

where $\Delta S_{\text{eff}} = \begin{cases} S_{\text{max}} - S_o & \text{for } S_o \geq S_{\text{min}} \\ S_{\text{max}} - S_{\text{min}} & \text{for } S_o < S_{\text{min}} \end{cases}$, and S_o is the crack opening stress.

Elber defined the effective SIF ratio, U , as,

$$U = \frac{\Delta K_{\text{eff}}}{\Delta K} = \frac{S_{\text{max}} - S_o}{S_{\text{max}} - S_{\text{min}}} = \frac{1 - \gamma}{1 - R} \quad (4)$$

where $\gamma = S_o / S_{\text{max}}$, and found that the effective SIF level to be a function of stress ratio for the 2024-T3 aluminium alloy. Using a simple polynomial function, he developed the following empirical relation for this material,

$$U = 0.5 + 0.4R. \quad (5)$$

Using the crack closure concept, the Paris law was reformulated as,

$$\frac{da}{dN} = C \Delta K^m = D \Delta K_{\text{eff}}^n = D (U \Delta K)^n \quad (6)$$

where D and n are the FCGR coefficient and exponent, respectively, correlating da/dN and ΔK_{eff} data. This shows that the FCGRs for different stress ratios may be expressed as a unique function of ΔK_{eff} . The result is significant as it indicates that the rate of fatigue crack growth for any combination of maximum and minimum applied stress, and loading history is uniquely characterised by ΔK_{eff} .

Since this original effort, the effective stress intensity formula for other common aircraft aluminium alloys were developed by researchers and are well documented in the open literature, e.g., [13]. However, all of these empirical equations indicate that U , and hence γ , are only a function of the stress ratio, R . Given this is the case, the FCGR exponents m and n , which are obtained by fitting the da/dN versus ΔK and da/dN versus ΔK_{eff} data, respectively, should remain identical. However, from a physics and mechanical perspective, U and γ must be functions of geometry and boundary conditions, and the applied stress. The crack opening stress equations, developed by Newman [14] based on analytical crack closure model calculations, provides these improvements for modelling γ and U .

2.4 Fatigue Crack Growth Rate Modelling

The Paris law does not account for the threshold range where long cracks stop growing and the limit range when catastrophic fracture is imminent. The FCGR equation, proposed by Newman [1], used in FASTRAN and CGAP is of the type,

$$da/dN = D(\Delta K_{\text{eff}})^n \frac{G}{H} \quad (7)$$

Here, D and n are the FCGR coefficient and exponent, respectively. G is a function of the threshold SIF range and the effective SIF range,

$$G = 1 - (\Delta K_0 / \Delta K_{\text{eff}})^2 \quad (8)$$

where ΔK_0 is the (long crack) threshold SIF range. If the applied SIF range is below the threshold SIF range, no crack growth takes place; hence it is a parameter to be determined experimentally, and is dependent on the material and the stress-ratio. Currently, there is a renewed interest in the values of the threshold SIF range, with the concern that the ones determined using the current ASTM load shedding test method may be too high [15]. If the applied effective SIF range is of the order of the threshold, the function G diminishes, thus reducing the FCGR to zero, simulating the threshold phenomenon. The function H , on the other hand, is a function of the maximum stress-intensity factor and the cyclic fracture toughness, defined as,

$$H = 1 - (K_{\text{max}} / C_5)^{C_6} \quad (9)$$

Here, C_6 is an empirical fitting parameter, and K_{max} is the maximum applied SIF. C_5 is the cyclic fracture toughness of the material. Clearly the function H diminishes as K_{max} approaches C_5 ; simulating the asymptotic behaviour of infinite FCGR as K_{max} approaches the critical SIF.

The addition of the G and H to the Paris law enables the sigmoidal shape in long FCGR data versus the SIF range to be simulated. Figure 4 demonstrates the FCGR equation used by CGAP and FASTRAN. Newman's crack opening stress equations [16], which are presented in the next section, were used to determine the crack opening stress. To provide some idea of the effect or sensitivity of the crack growth curve due to S_{max}/σ_0 and R values, four FCGR curves for four combinations of S_{max}/σ_0 and R values were shown in Figure 4. Here, σ_0 is the flow stress, which is the average of the uniaxial yield stress σ_y and the ultimate stress σ_u . The results in Figure 4 indicate that while the load interaction effects on FCGR data within the Paris regime can be rationalized using ΔK_{eff} , it is unable to do so for FCGR data in region III. This is because C_5 , or K_C , is not affected by load interaction effects. Therefore, the idea that long FCGR data is uniquely characterised by ΔK_{eff} only applies to region II (the Paris regime), and partially, in region I due to the possible presence of other mechanisms affecting the threshold ΔK_{eff} value.

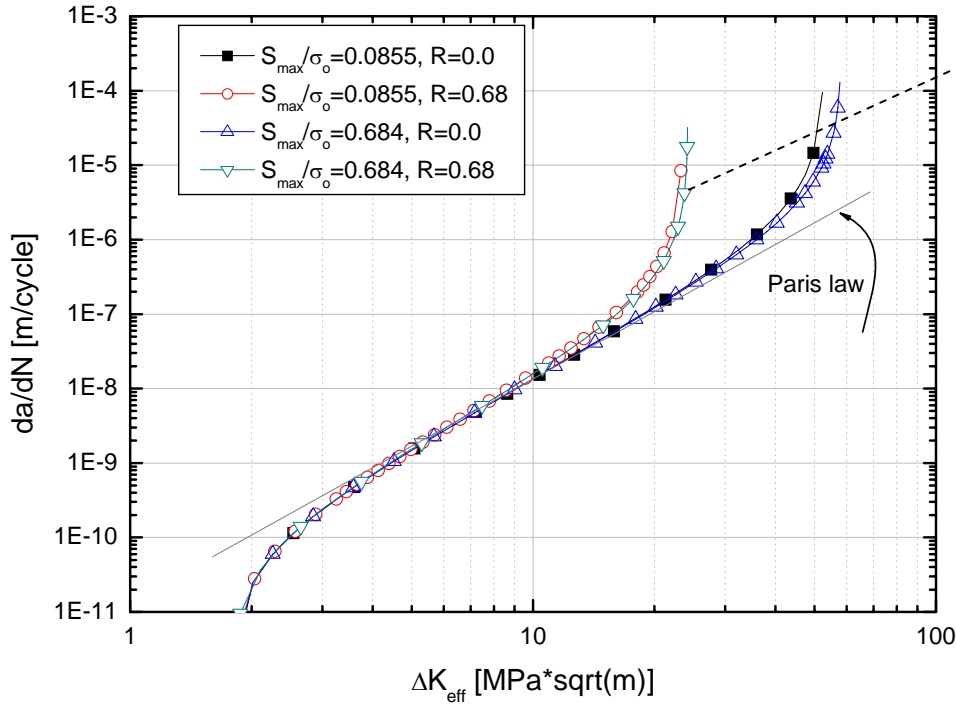


Figure 4: The effect of S_{\max}/σ_0 and R on FASTRAN (and CGAP) FCGR model

The parameters used to compute this example were $D = 4 \times 10^{-10}$, $n = 3$, $\Delta K_0 = 1.95$, $C_5 = 82$ and $C_6 = 2$.

2.5 Elastic-Plastic Effective Stress Intensity Factors

The ΔK_{eff} concept developed by Elber (1971) and discussed in the previous sections was based on linear elastic analyses. However, this is inadequate during proof loading or near failure where the stress intensity is large and the plastic zone size is significant. To allow for plasticity, part of the monotonic plastic zone size ρ could be added to the crack length a . Therefore, Equation (3) may be modified to give an elastic-plastic effective SIF [16],

$$\Delta \bar{K}_{\text{eff}} = F(d) \Delta S_{\text{eff}} \sqrt{\pi d} \quad (10)$$

where,

$$d = c_x + \omega/4 \quad (11)$$

c_x is the current crack length a plus the FCGR (da/dN) per one cycle and ω is the closure corrected cyclic plastic zone size. The plasticity correction of $\omega/4$ was derived in [16] and according to Newman [16], it requires further experimental and analytical verification. Note that the geometry-boundary correction factor F should be determined using the crack length d . The closure corrected cyclic plastic zone size is approximated by:

$$\omega = \rho/4(1 - R_{\text{eff}})^2 \quad (12)$$

where ρ is the monotonic plastic zone size and R_{eff} is the ratio of crack opening stress to the maximum stress. The monotonic plastic zone size, ρ , for a centre crack tension (CCT) specimen was provided in [16] and is shown below:

$$\rho = a \left\{ \left(\frac{2W}{\pi a} \right) \arcsin \left[\sin \left(\frac{\pi a}{2W} \right) \sec \left(\frac{\pi S f}{2 \alpha \alpha_0} \right) \right] - 1 \right\} \quad (13)$$

where $f = 1 + 0.22(a/W)^2$ and S is the maximum stress, W is the width of the specimen.

Newman [16] has also proposed other forms of equations to approximate the elastic-plastic crack length d , such as

$$d = c_x + \rho/4 \quad (14)$$

$$d = c_x + \rho \quad (15)$$

Note that Newman recommends that elastic-plastic SIFs should only be used for proof testing or severe loading (such as low cycle fatigue conditions) [16]. Most crack growth analyses can be performed using linear elastic effective SIFs.

3. Newman's Crack Opening Stress Equations

Newman's crack opening stress equations are implemented in FASTRAN, CGAP and AFGROW for estimating crack opening stresses for CCT specimens subjected to constant amplitude loading. Also based on polynomial functions, Newman [17] developed this set of crack opening stress equations, using numerical crack closure results for the (CCT) specimen, as a function of maximum stress level, S_{max}/σ_0 , geometry and boundary correction factor, $F(a)$, and constraint factor, α ,

$$S_o / S_{\text{max}} = \begin{cases} A_0 + A_1 R + A_2 R^2 + A_3 R^3, & \text{for } R \geq 0, \\ A_0 + A_1 R, & \text{for } R < 0. \end{cases} \quad (16)$$

where the coefficients in Equation (16) are given as,

$$\begin{aligned} A_0 &= (0.825 - 0.34\alpha + 0.05\alpha^2) [\cos(\pi F(a) S_{\text{max}} / 2\sigma_0)]^{1/\alpha} \\ A_1 &= (0.415 - 0.071\alpha) F(a) S_{\text{max}} / \sigma_0 \\ A_2 &= 1 - A_0 - A_1 - A_3 \\ A_3 &= 2A_0 + A_1 - 1 \end{aligned} ,$$

α is the constraint factor and $F(a)$ is the crack geometry and boundary correction factor.

If the crack opening stress calculated from this equation is smaller than the minimum stress, S_{min} , of the load cycle, then $S_o = S_{\text{min}}$. For convenience, the geometry-boundary

correction factors $F(a)$ for the centre-crack tension and compact tension specimens are shown below in Equations (19) and (21), respectively. These types of specimens are normally used for FCGR characterisation.

Newman in [16] also developed a crack opening stress equation for a compact tension (CT) specimen. The solution takes the same form as Equation (10) except that S_{max} is replaced with S'_{max} (for $R \geq 0$) which is defined as, based on the equivalence of SIF for the two types of specimens,

$$S'_{max} = \frac{P}{Wt} \frac{F_{CT}}{F_{CCT}} \quad (17)$$

where P is the applied load, W is the width of the specimen, t is the thickness of the specimen and F_{CT} and F_{CCT} are the geometry-boundary correction factors for CT and CCT specimens respectively.

In FASTRAN II [16], the crack opening stress was further modified to account for large crack growth increments (relative to the crack length). The modified crack opening stress (S'_o) equation for constant amplitude loading is given by:

$$S'_o = S_o - 0.3\sigma_0 \sqrt{\Delta a/a} / F(a) \quad \text{for } S_{max}/\sigma_0 < 0.6 \quad (18)$$

where S_o is the crack opening stress from Equation (16), Δa is the crack growth increment (or rate per cycle), and a is the current crack length. The difference between S'_o and S_o becomes significant (more than 2%) for growth rates greater than about 10^{-5} m/cycle. For $S_{max}/\sigma_0 > 0.6$, the crack opening stress should be determined by analysis using CGAP (or FASTRAN II) with the geometry of the test coupon.

This set of crack opening stress equations is very attractive in that the only unknown in these equations is the constraint factor ' α '. As a result, this set of crack opening stress equations is widely used today, in particular in FASTRAN II [16], CGAP, AFGROW [2] and the Flight-Life module of DARWIN [18], for estimating crack opening stresses.

3.1 Centre-Crack Tension (CCT) Specimen

For the centre-crack tension specimen, S is the remote applied stress. $F(a)$ for the centre-crack tension specimen, i.e. F_{CCT} , is given by,

$$F(a) = \sqrt{\sec\left(\frac{\pi a}{2W}\right)} \quad (19)$$

where a is the half crack length and W is the half total width of the specimen.

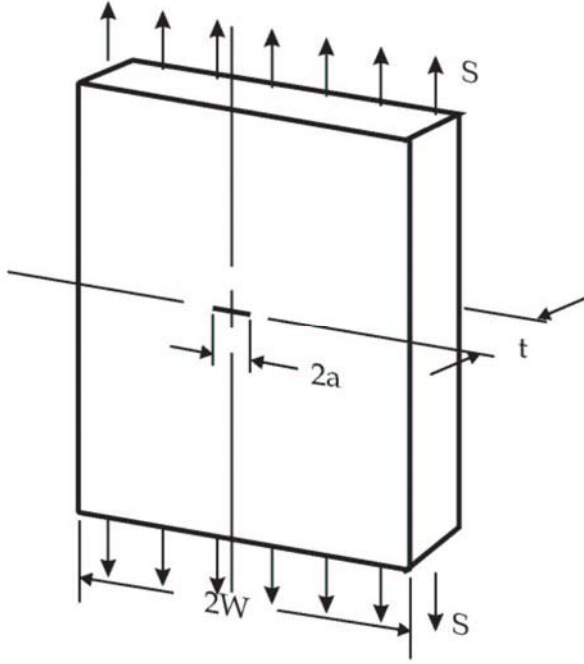


Figure 5: Centre Crack Tension (CCT) specimen

3.2 Compact Tension (CT) Specimen

For the compact tension specimen, S is defined as,

$$S = \frac{P}{tW}, \text{ so } S_{\max} = \frac{P_{\max}}{tW}. \quad (20)$$

$F(a)$ for the compact tension specimen, i.e. F_{CT} , is given by,

$$F(a) = \left[0.886 + 4.64\lambda - 13.32\lambda^2 + 14.72\lambda^3 - 5.6\lambda^4 \right] \frac{(2 + \lambda)}{(1 - \lambda)^{3/2}} \frac{1}{\sqrt{\pi\lambda}} \quad (21)$$

Here $\lambda = \frac{a}{W}$, W and t are the width and the thickness of the specimen, respectively.

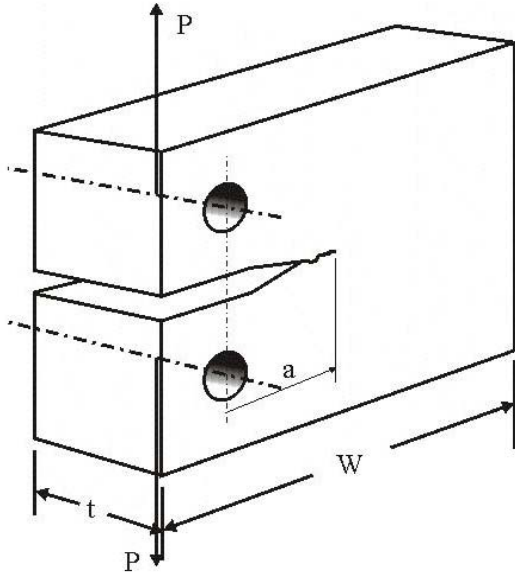


Figure 6: Compact Tension (CT) specimen

3.3 Limitations

From a mathematical point of view, the crack opening stress equations are limited to,

$$0 \leq \frac{F(a)S_{\max}}{\sigma_0} < 1 \quad (22)$$

However, genuine da/dN versus ΔK data would not exceed this condition because fracture of the specimen would have occurred prior to $F(a)S_{\max}/\sigma_0$ exceeding unity.

For various R values, $\gamma = S_o/S_{\max}$ for the compact tension and the centre-crack tension specimens are plotted in Figure 7 and Figure 8, respectively. As illustrated, this set of crack opening stress equations are a function of the crack geometry-boundary and the maximum applied stress level S_{\max}/σ_0 . For long cracks, γ remains reasonably constant for $\lambda > 0.1$ to $\lambda \approx 0.5$. Outside this range, the shift or conversion from ΔK to ΔK_{eff} are sensitive to geometry. This indicates that the FCGR exponents m and n , Equation (6), are not the same, but their differences diminish as ΔK approaches ΔK_{eff} , i.e. at high R values where the effect of crack closure is small. It is important to be aware of this to avoid utilising the incorrect FCGR parameter for the FCGR prediction model.

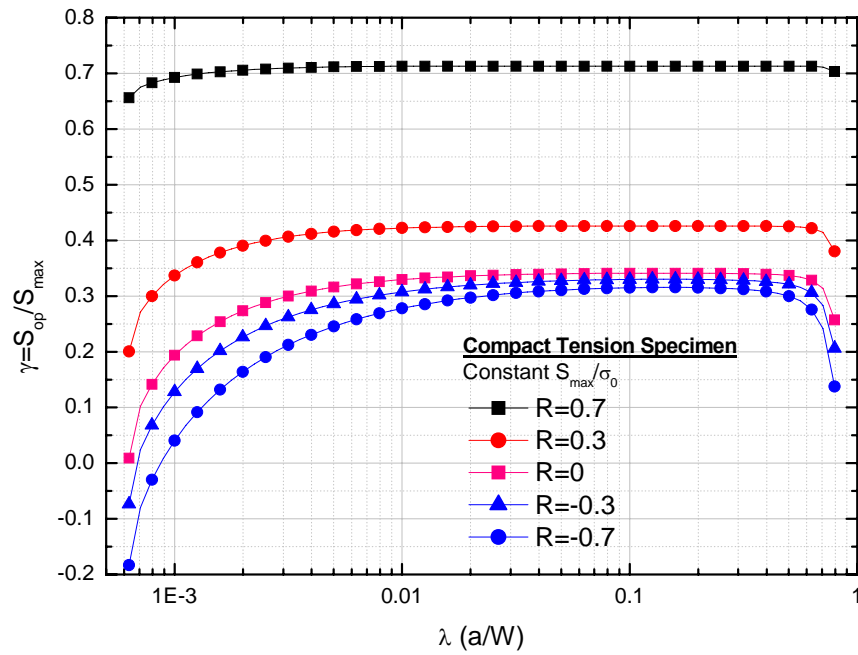


Figure 7: The effect of R ratio and crack length on crack opening stress levels for compact tension specimens

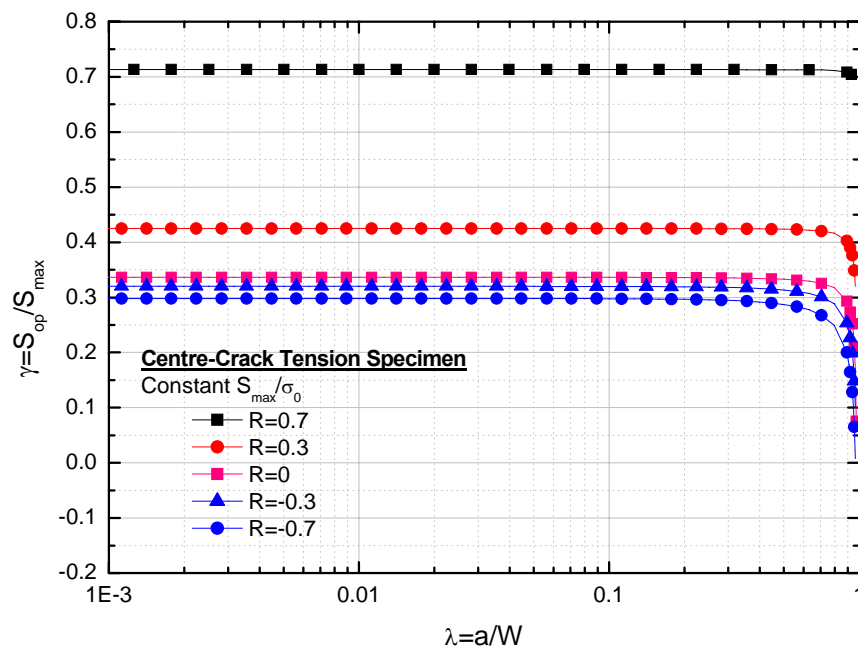


Figure 8: The effect of R ratio and crack length on crack opening stress levels for centre crack tension specimens

4. DKEFF Program and CGAP Crack Growth Rate Conversion Module

The DKEFF program [16] was the original software code developed by Newman to perform the conversion from da/dN versus ΔK data at multiple R ratios to a single curve of da/dN versus ΔK_{eff} using Equation (16), but its text-based often makes the analysis a daunting task. For this reason, the DKEFF program has been modified, enhanced and incorporated with CGAP to make use of the attractive GUI of CGAP for enabling the process of FCGR conversion to be carried out simply and intuitively. Shown in Figure 9 is a view of the CGAP FCGR conversion module's mostly used window – the “Material” tab window.

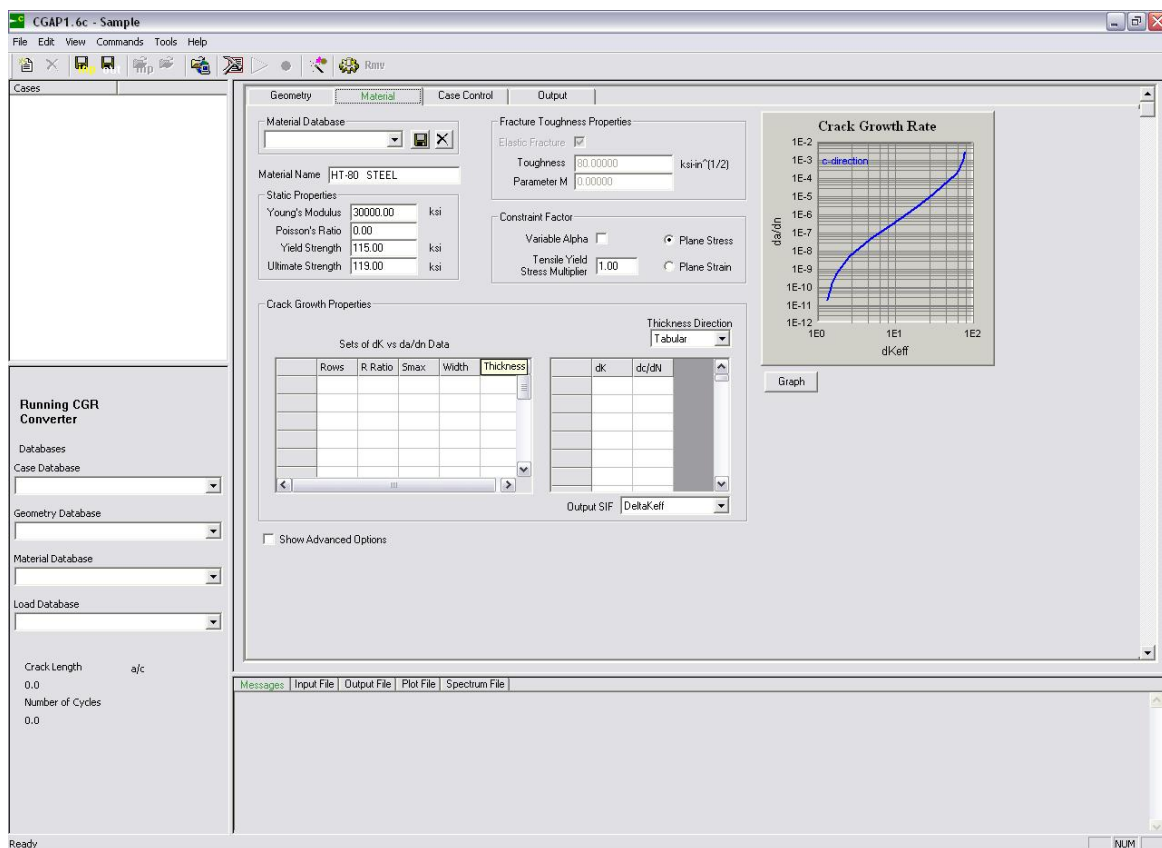


Figure 9: CGAP's FCGR conversion module's main “Material” tab window

Further module views and the use of the CGAP FCGR conversion module are documented in Appendix C, together with additional examples to clarify the methodology. Appendix A also includes a flowchart of the basic operations, how to run FCGR conversion module and a summary of the major inputs required by the CGAP FCGR conversion module. The steps which are followed by the DKEFF program and now the CGAP's FCGR conversion module, the use of constant α and variable α options and some examples of results using CGAP's FCGR conversion module are presented in this section.

4.1 Effective Stress Intensity Factor Calculation

Given ΔK , R and α , computing ΔK_{eff} using the DKEFF program or the CGAP FCGR conversion module, requires several additional test and geometry parameters as input. They are S_{max} (or P_{max} for CT specimen), the specimen type (CT or CCT) and the width, W , for each da/dN versus ΔK data set. With these input data and given the value of α , the following steps are followed to determine the ΔK_{eff} value for each combination of ΔK - R values, and ultimately, the optimum constraint factor.

1. Obtain the crack size, a , by finding the solution to the equation,

$$F(a)\sqrt{\pi a} = \frac{\Delta K}{\Delta S} \quad (23)$$

2. Calculate $F(a)$.
3. Calculate the coefficients in the crack opening stress equations, Equation (16).
4. Compute the crack opening stress level γ
5. Use Equation (4) or (10) to obtain ΔK_{eff} or $\overline{\Delta K}_{\text{eff}}$, respectively.

An iterative approach may be used to solve the non-linear equation in Step 1. Also note that the FCGR conversion module outputs both the elastic and elastic-plastic effective SIF ranges versus da/dN data.

The DKEFF and FCGR conversion module requires that the FCGR data are obtained from the same type of either CT or CCT specimens. It presently does not allow FCGR data from both types of specimens to be mixed for conversion. It is important that the user correctly selects the type of specimen according to the data in the “Geometry” tab window during set up.

The da/dN and ΔK_{eff} data need to be plotted, in a double logarithmic scale, to visually examine how well the selected value of α performed in collapsing the multiple R da/dN - ΔK data. In the CGAP FCGR conversion module, this plotting can be done directly and immediately within the GUI.

4.2 Constant Constraint Factor

Since FCGR for long cracks is believed to be uniquely characterised by ΔK_{eff} , the optimum α is the α value that best collapses the da/dN versus ΔK data, within the Paris regime, for a range of R values to a single da/dN versus ΔK_{eff} curve. A trial and error approach is required to obtain this optimum value of α .

Despite α being used as a fitting parameter for converting da/dN versus ΔK data to da/dN versus ΔK_{eff} , there are some physical constraints on what value it may take. Firstly, the optimum α must provide a da/dN versus ΔK_{eff} curve that lies relatively close to the da/dN versus ΔK curves for high R (0.7 and above) values. This is because ΔK

approaches ΔK_{eff} as R increases, and it has been demonstrated that crack surface closure ceases at R of approximately 0.7 [19]. Secondly, the optimum value of α must be between 1 and 3 [16], from the argument that α acts as a multiplier to the uniaxial yield stress to account for the effect of non-uniaxial stress state. It cannot be less than 1 for the plane stress condition, and it cannot be greater than 3 for the plane strain condition. It should be common practice to check that the optimum α value satisfies these two criteria.

The constant α option is activated by default, and it is confirmed when the Variable Alpha checkbox is unchecked. This is shown in Figure 10.

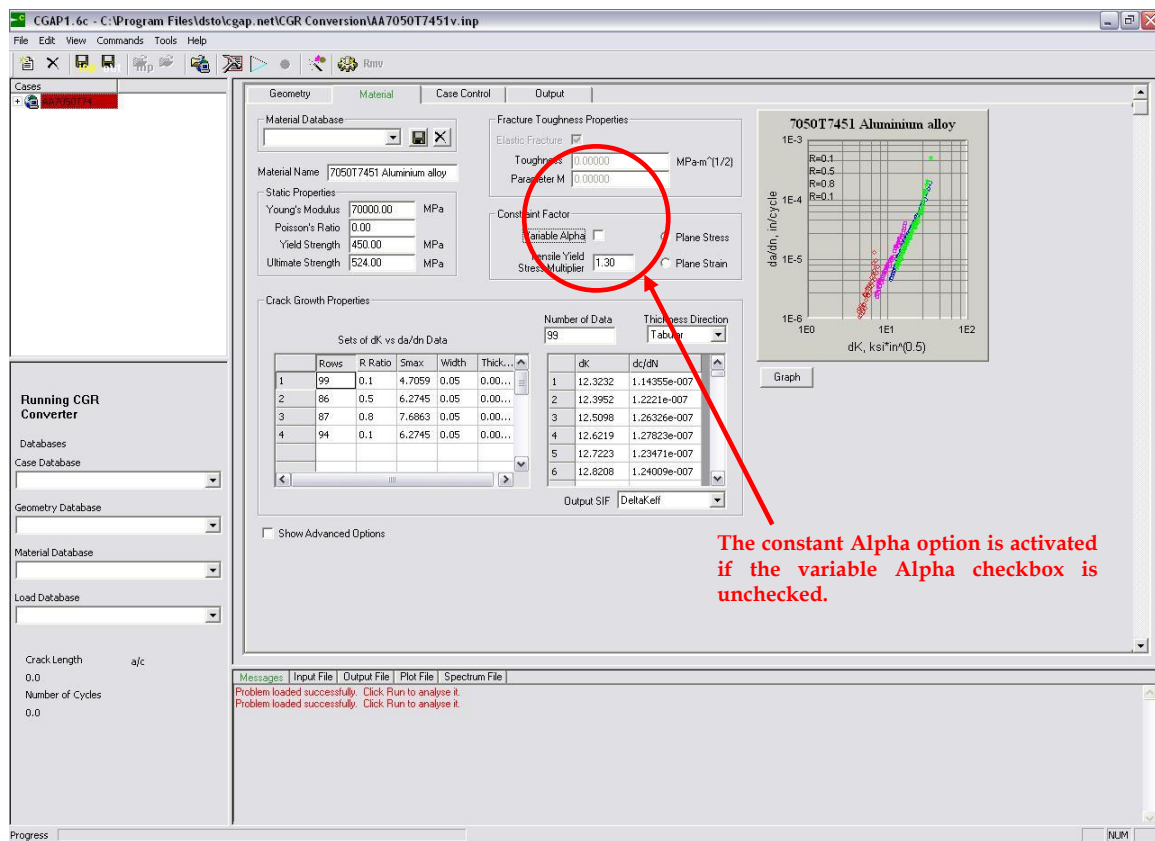


Figure 10: Selecting the constant α option

4.3 Variable Constraint Factor

In the above (constant α) case, a single value of α was applied to the entire range of the FCGR data. The constraint factor, α , (or stress state) however, may not be constant for reasons such as (i) a change of stress state as the crack length and FCGR increases or (ii) a change in crack geometry or (iii) a change in crack growth mechanisms. From a fitting parameter perspective, varying α can also be used as a means for better collapsing the da/dN versus ΔK data to a unique da/dN versus ΔK_{eff} curve. Irrespective of the underlying reason for a varying α condition, the FCGR conversion module in CGAP (or DKEFF) allows this effect to be taken into account via the variable α option, as shown in Figure 11.

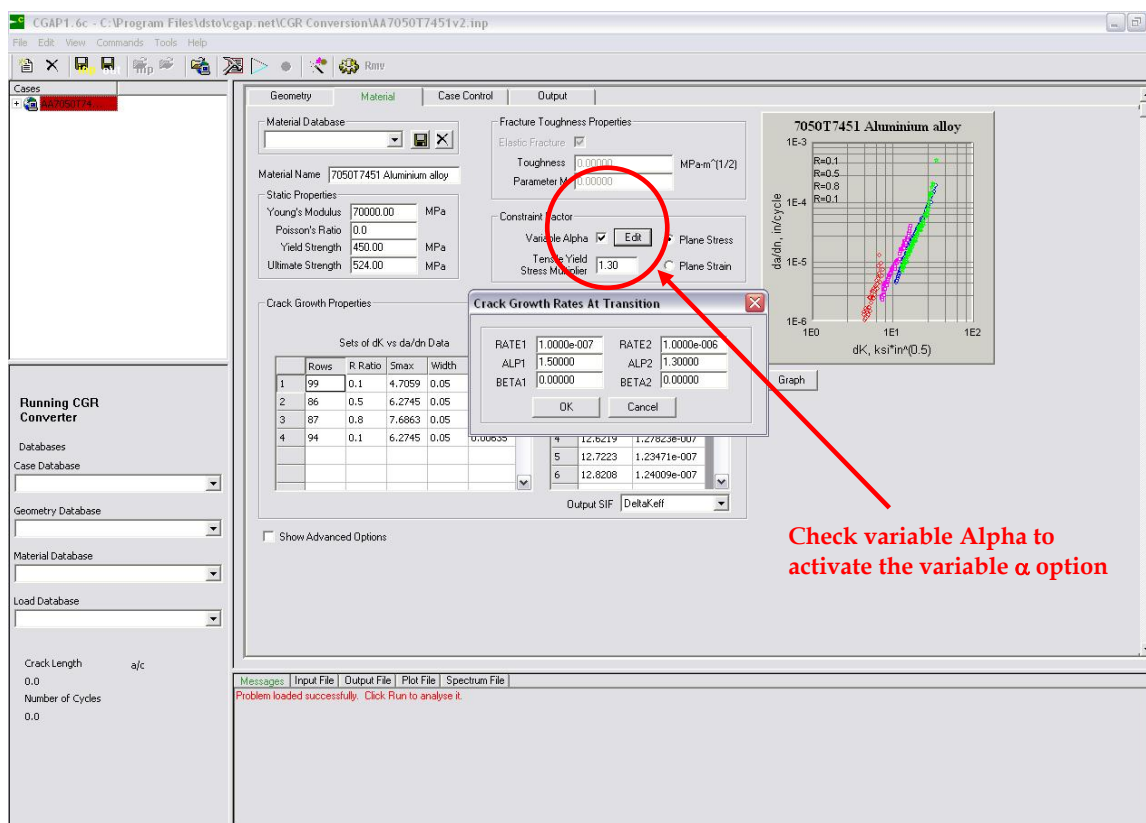


Figure 11: Variable α option and parameters input dialog box in the FCGR conversion module

When this option is selected, two values of α (α_1 and α_2) need to be assigned to two different FCGRs (da/dN_1 and da/dN_2). These input parameters separate the FCGRs into three segments as illustrated in Figure 12. For rates less than da/dN_1 , the crack opening stress equation uses α_1 , and for rates greater than da/dN_2 , α_2 is used. For the middle segment between da/dN_1 and da/dN_2 , α varies linearly from α_1 to α_2 . According to Newman [16], the first α and its associated rate represents the regime near the start of the constraint loss while the second α and rate represents the regime near the end of constraint loss. This is linked to the transition from flat to slant crack growth in some materials [16] (or generally from a change of crack geometry or crack growth mechanisms) or the change from a more plane strain condition at a low ΔK_{eff} value to a more plane stress condition at a high ΔK_{eff} value.

In order to utilise the variable constraint factor option, the conditions that $\alpha_1 > \alpha_2$ and $da/dN_1 < da/dN_2$ must be satisfied. These restrictions were built into DKEFF and subsequently preserved in the CGAP FCGR conversion module because the crack tip stress state must be at least equal to or more than the plane strain at a lower growth rate than higher growth rate. It should be noted that the condition that α (α_1 and α_2) must be

within the range of 1 and 3 still applies for the variable α option. A sufficient transition FCGR range should be given to allow a smooth transition from α_1 to α_2 .

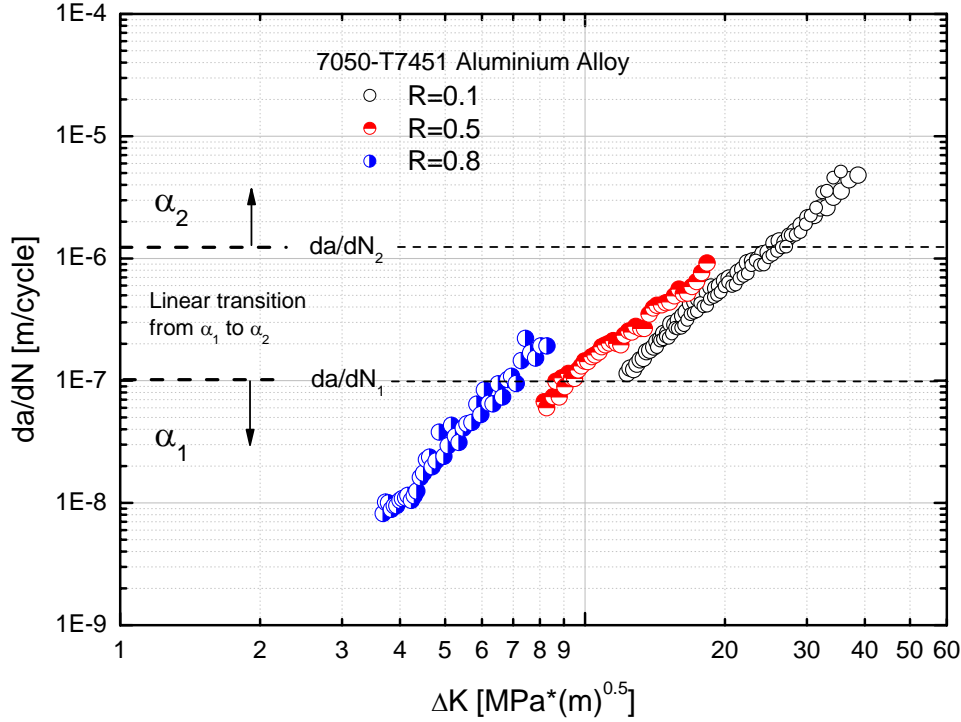


Figure 12: Schematic illustration of the inputs α_1 , α_2 , da/dN_1 and da/dN_2 for the variable α option

5. Examples

To activate the FCGR conversion module implemented in CGAP, the user must start CGAP and select FCGR converter in the settings dialog box that is found under the *tools* menu in *Configuration....* This is shown in Figure A.2. Refer to the user guide in Appendix A for more detailed information on the use of the FCGR converter program. The location and file names for the following examples are given in Appendix C.

5.1 7050-T7451 Aluminium Alloy Example

Two examples are presented in this subsection, both utilising the 7050-T7451 aluminium alloy da/dN versus ΔK data previously shown in Figure 3 (or Figure 12) to demonstrate the procedure to convert da/dN versus ΔK at multiple R values to da/dN versus ΔK_{eff} . The first example uses a constant constraint factor and the second uses variable constraint factors, to demonstrate the effect of α in Newman's crack opening stress equations.

The 7050-T7451 aluminium alloy crack growth tests were carried out using compact tension specimens. Table 1 contains the test and geometry parameters for the 7050-T7451 FCGR data that is necessary for the conversion procedure.

Table 1: Test load and geometry parameters for the 7050-T7451 aluminium alloy specimens FCGR data in Figure 3

Specimen	P_{\max} (KN)	R	W (m)	t (m)	σ_0 (MPa)
1	4.7059	0.1	0.05	0.00635	450
2	6.2745	0.5	0.05	0.00635	450
3	7.6863	0.8	0.05	0.00635	450
4	6.2745	0.1	0.05	0.00635	450

5.1.1 Constant Constraint Factor

Figure 13 to Figure 16 present the da/dN versus ΔK_{eff} plots for $\alpha = 1, 1.3, 2$ and 3 , respectively. The original da/dN versus ΔK data are plotted in grey in the background to illustrate the differences in the change from ΔK to ΔK_{eff} due to the effect of R values and changes in α .

This series of plots provides a clear visualisation of the effect of α on Newman's crack opening stress equations, and the shift of the ΔK values to their corresponding ΔK_{eff} values.

Higher values of α indicate a plane strain condition and hence, lower amounts of plastic deformation at the crack tip than resides along the crack surface. Therefore, a high α value is more suitable for FCGR data that has low sensitivity to the R ratio effect.

It should be noted that the da/dN values do not change; only the ΔK values are reduced (due to the presence of plasticity-induced crack closure) to their corresponding ΔK_{eff} value. Note that the ΔK_{eff} value is always less than or equal to the associated ΔK value.

The best collapse of the 7050-T7451 da/dN versus ΔK data, based on R^2 value (or coefficient of determination, see Appendix B), was achieved at an $\alpha = 1.3$, as shown in Figure 14. Despite the fact that the data collapsed best at this α value, Figure 14 showed that the ΔK values for FCGRs at $R = 0.8$ were not the ΔK_{eff} values. This is seen in Figure 14 by the small shift in the ΔK data at $R = 0.8$ to the ΔK_{eff} data. This result is physically inconsistent with the suggestion that $R \approx 0.7$ is the threshold for crack closure (surface contact).

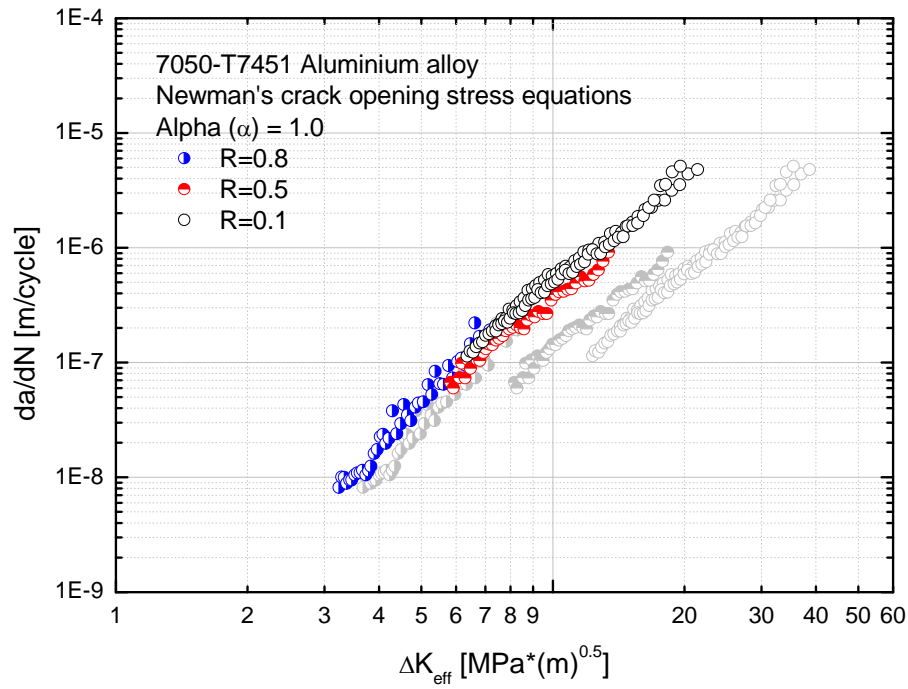


Figure 13: da/dN versus ΔK_{eff} data for $\alpha = 1$

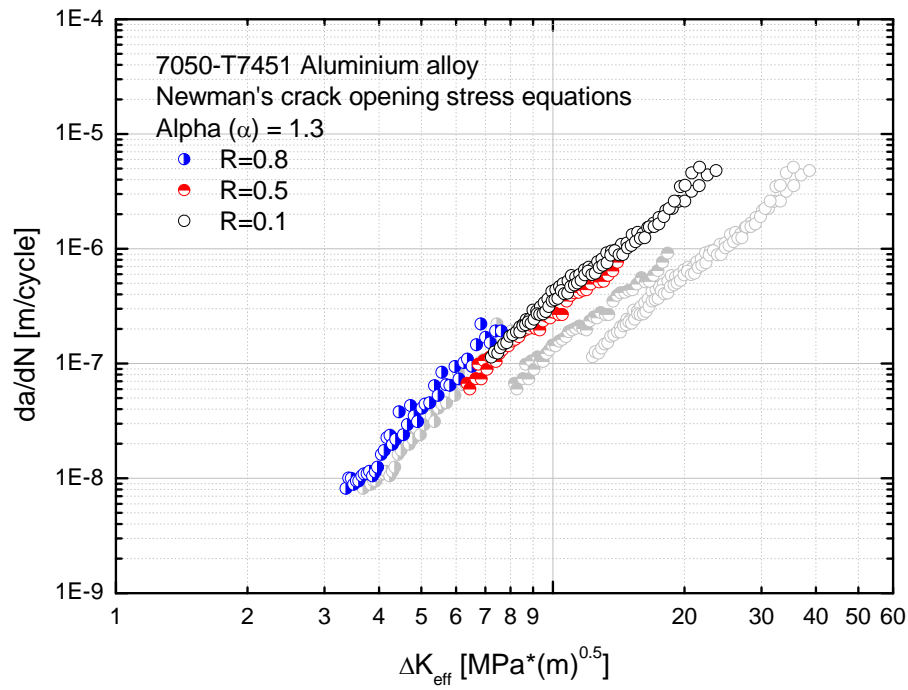


Figure 14: da/dN versus ΔK_{eff} data for $\alpha = 1.3$

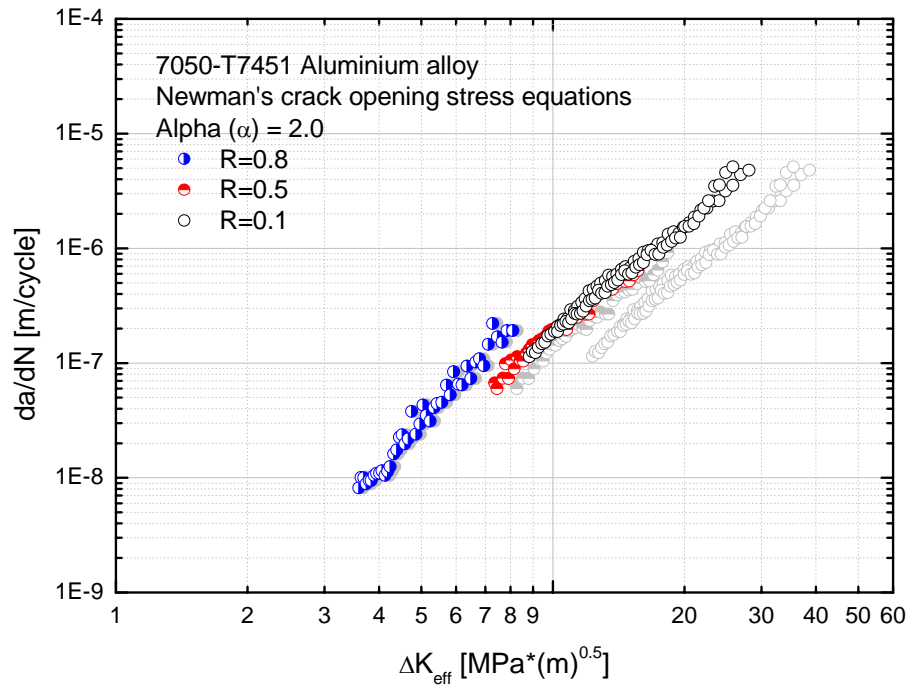


Figure 15: da/dN versus ΔK_{eff} data for $\alpha = 2$

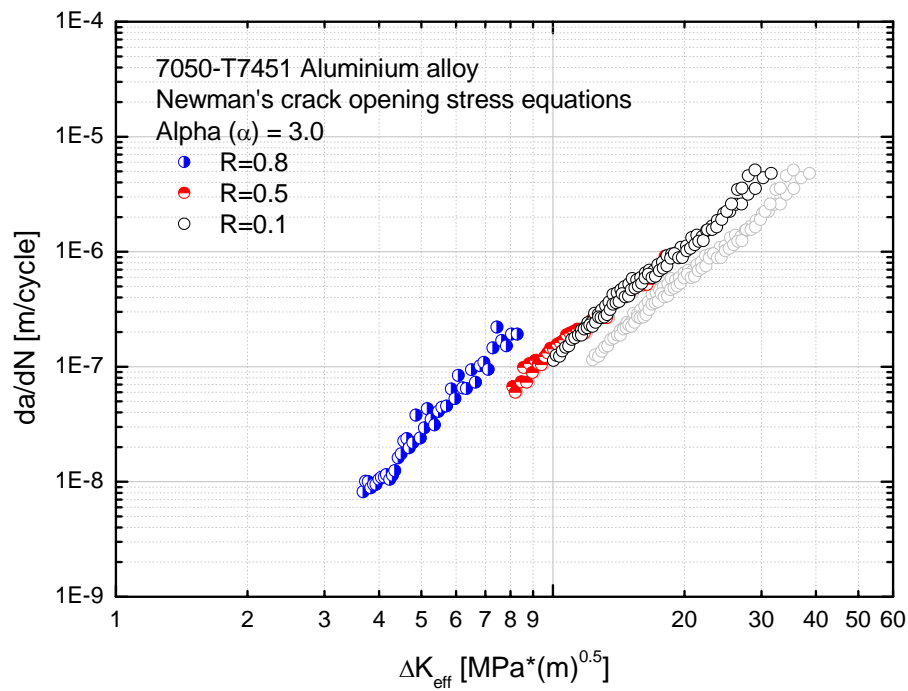


Figure 16: da/dN versus ΔK_{eff} data for $\alpha = 3$

5.1.2 Variable Constraint Factors

As shown by the examples in Section 5.1.1 (constant α), the optimum constant value of α is 1.3 for this set of FCGR data. However, it was shown in Figure 14 that this value of α suggests plasticity-induced crack closure is present even at $R = 0.8$. This is somewhat inconsistent with the understanding that plasticity-induced crack closure is only observed for $R \leq 0.7$ [19]. This example was designed to overcome this inconsistency purely via fitting the FCGR data using the variable α option, and no physical reason for the variation in α was considered. In order to minimise the shift in the FCGR data at the R value of 0.8 (data shown in blue), the α value must be increased to reduce the effect of crack closure. The input parameters, α_1 , α_2 , da/dN_1 and da/dN_2 selected for the variable α option are displayed in Figure 17 with the FCGR conversion module results. Plotted in grey in the background of these figures are again the original da/dN versus ΔK data to allow the change from ΔK to ΔK_{eff} values to be observed.

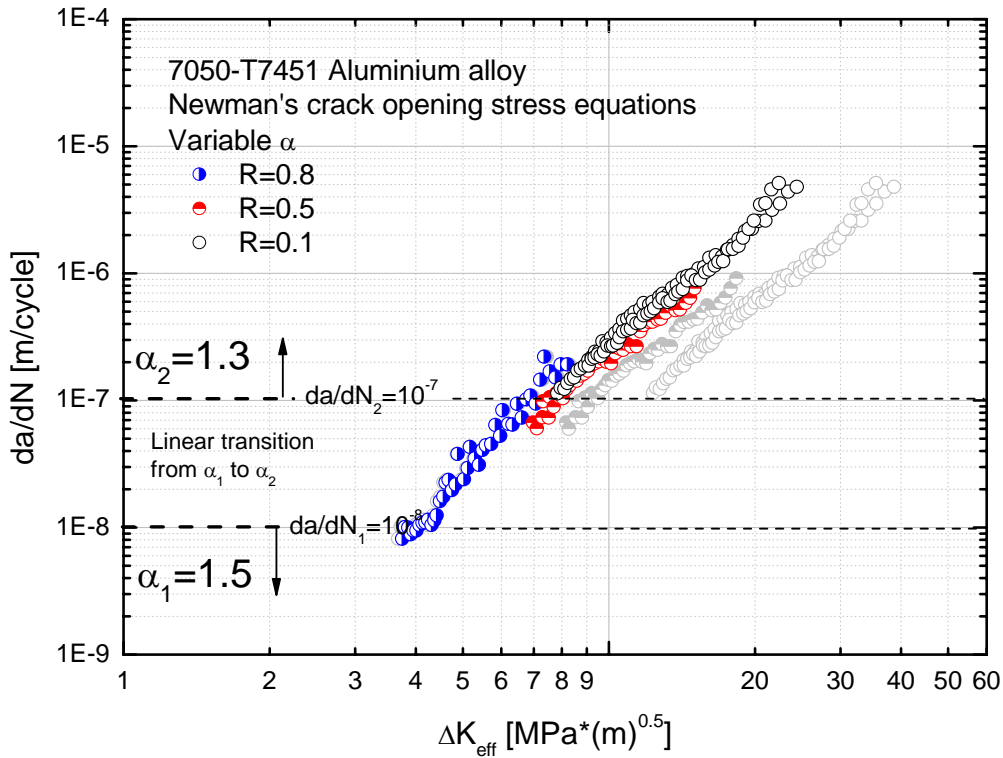


Figure 17: Variable α example: $\alpha_1 = 1.5$, $\alpha_2 = 1.3$, $da/dN_1 = 10^{-8}$ and $da/dN_2 = 10^{-7}$

As shown in Figure 17, optimising α_1 and α_2 resulted in a significant improvement to the results from $\alpha = 1.3$. In particular, the predicted $da/dN - \Delta K_{\text{eff}}$ data at $R = 0.8$ are now almost identical to $da/dN - \Delta K$ data, and visually all of the FCGR data also collapsed just as well as compared to that shown in Figure 14.

5.2 2219-T851 Aluminium Alloy Example

Two more examples are presented utilising 2219-T851 aluminium alloy da/dN versus ΔK data, shown in Figure 18. These data were obtained from Reference [20]. Example 1 presents the constant constraint factor case and example 2 is the variable constraint factor case.

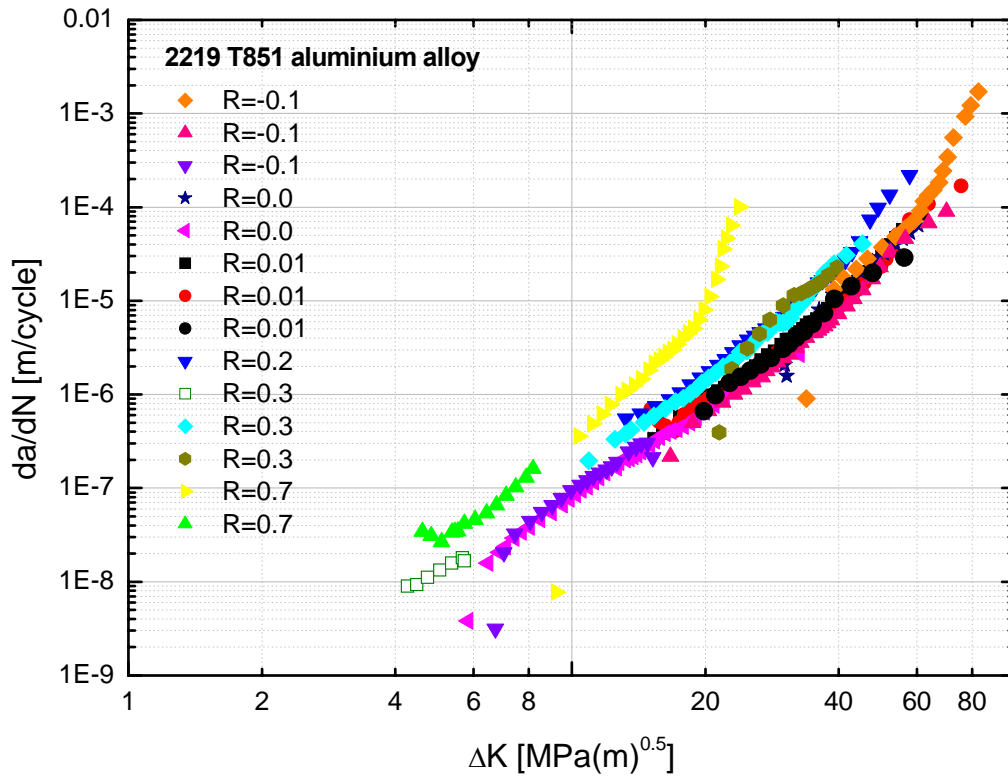


Figure 18 2219-T851 aluminium alloy da/dN versus ΔK data from Ref. [20]

The tests were carried out on centre crack tension (CCT) specimens. Table 2 contains the test and geometry parameters for the FCGR data required for the conversion procedure.

Figure 19 and Figure 20 display the da/dN versus ΔK_{eff} data for the constant constraint factor and the variable constraint factor cases, respectively. Again, plotted in grey in the background of these plots are the original da/dN versus ΔK data shown in Figure 18 thus allowing easy examination of the results of the FCGR conversion process.

Table 2 Test stress and geometry parameters for the 2219-T851 aluminium alloy specimens
FCGR data from Ref. [20]

Specimen	S_{\max} (MPa)	R	W (m)	t (m)	σ_0 (MPa)
1	138	0.01	0.0762	0.00635	406.5
2	138	0.01	0.0762	0.00635	406.5
3	138	0.7	0.0762	0.00635	406.5
4	138	0.2	0.0762	0.00635	406.5
5	138	0.3	0.0762	0.00635	406.5
6	55.2	0.7	0.0762	0.00635	406.5
7	275.8	0.3	0.0762	0.00635	406.5
8	275.8	0.0	0.0762	0.00635	406.5
9	275.8	0.7	0.0762	0.00635	406.5
10	55.2	-0.01	0.0762	0.00635	406.5
11	138	-0.01	0.0762	0.00635	406.5
12	275.8	-0.01	0.0762	0.00635	406.5
13	55.2	0.3	0.0762	0.00635	406.5
14	138	0.01	0.0762	0.00635	406.5

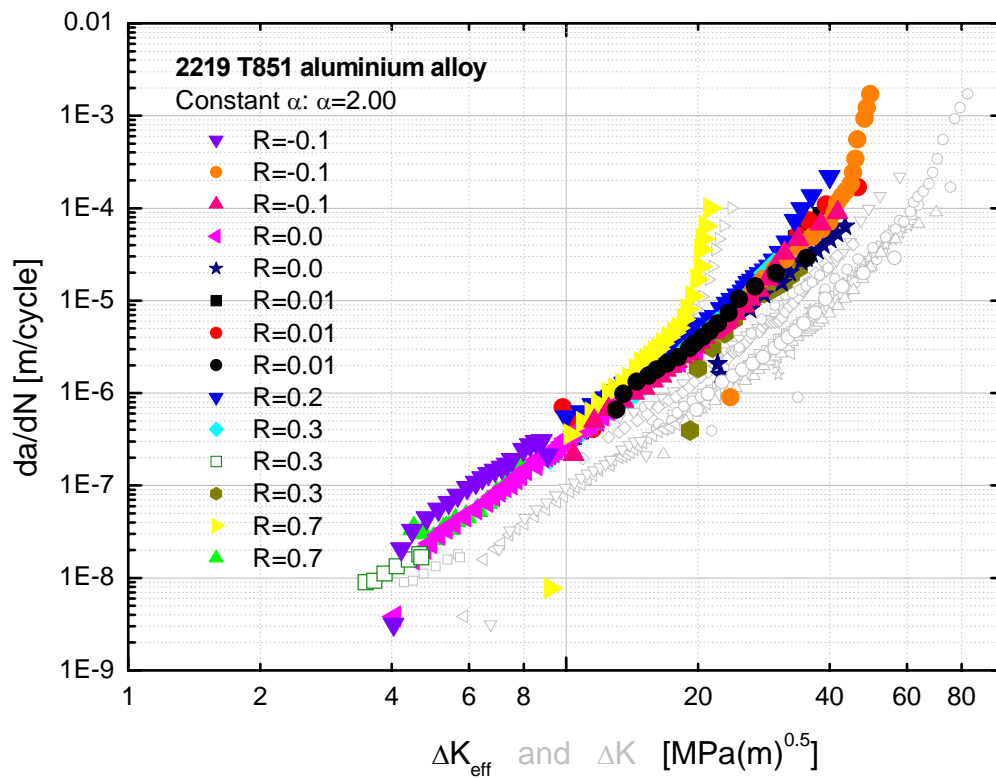


Figure 19 2219-T851 al. alloy constant α example: optimum $\alpha = 2.0$

5.2.1 Constant Constraint Factor

For the constant constraint factor case, the optimum value of α , based on visual examination, is 2.0, and the result is shown in Figure 19.

5.2.2 Variable Constraint Factor

For the variable constraint factor case, the optimum collapse, based on the authors' judgement, of the FCGR data is shown in Figure 20. An α of 2.3 (α_1) was selected for FCGR below 10^{-7} m/cycle (da/dN_1), and an α of 1.73 (α_2) was selected for FCGR above 10^{-6} m/cycle (da/dN_2). These are also shown in Figure 20.

Comparing to the case of constant α , the variable constraint factor was able to better collapse the FCGR data for the whole range of FCGR data.

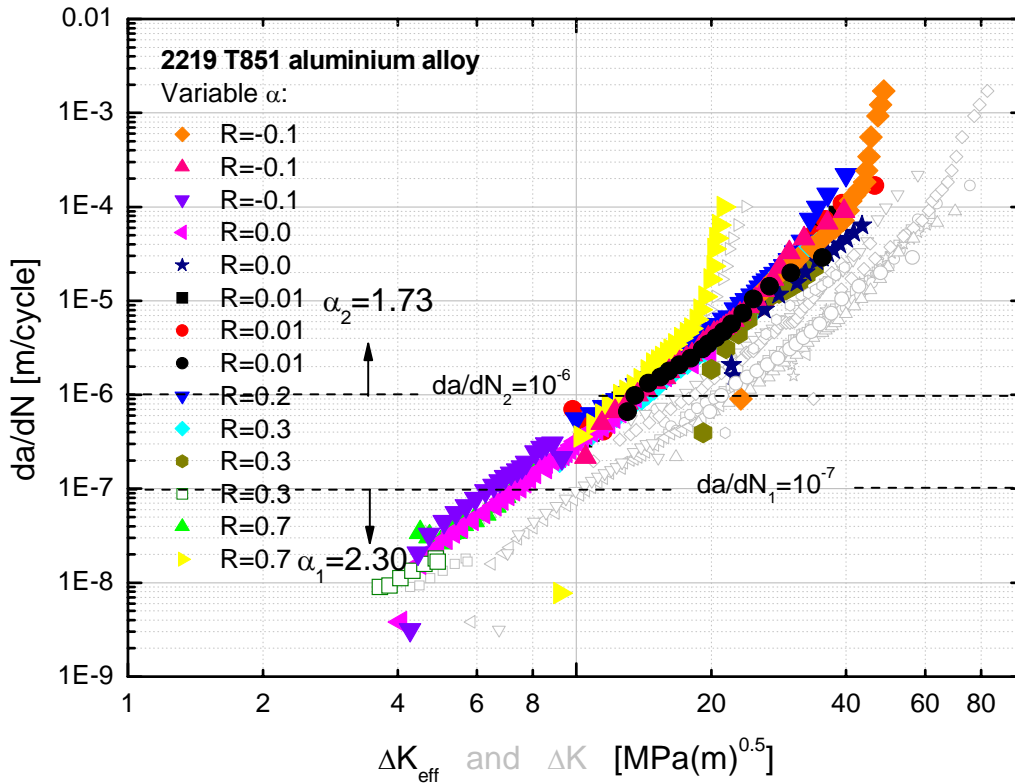


Figure 20 2219-T851 al. alloy variable α example: $\alpha_1 = 2.3$, $\alpha_2 = 1.73$, $da/dN_1 = 10^{-7}$ and $da/dN_2 = 10^{-6}$

6. Discussion

6.1 Finding the Optimum Constraint Factor

A unique (constant) value of α that allows the FCGR data with various R values to be collapsed onto a single curve is very attractive due to its simplicity. For this and practicality reasons, it is recommended that FCGR conversion should initially be carried out using the constant α option in CGAP. It is important to observe the physical limits of α that were mentioned in Section 4.1.

To aid this process, it is desirable that a means for quantitatively measuring how well the data collapsed onto a unique line is available. The coefficient of determination for example, as shown in Appendix B, could potentially meet this need. This, however, is something that needs to be pursued in the near future through the ongoing support effort planned for CGAP.

Once an indicative α has been obtained the analysis should be switch to the variable α option to optimise the collapse of the FCGR data. This second process provides a logical approach to obtaining the best collapse of the FCGR data, and could minimise the amount of trial and error on the value(s) of α before arriving at a final da/dN versus ΔK_{eff} curve.

6.2 Limitations

Sections 2-4 have discussed the concept of plasticity-induced crack closure, crack opening stress, the constraint factor, α , and the plasticity-corrected SIFs. As discussed in these sections, the basis of this work such as the plasticity-induced crack closure model and crack opening stress equations are based on LEFM. However, since the crack closure phenomenon and the effective SIF concept accounts for the effect of the non-linear permanent plastic deformation in the vicinity of the crack tip, ΔK_{eff} can be considered as an elastic-plastic fracture mechanics parameter. Indeed, the use of the ΔK_{eff} concept has significantly extended the limits of LEFM in both large-scale yielding [21, 22] and the mechanically short crack [21, 23-25] regimes compared to the use of the nominal ΔK .

The crack closure model considered in this investigation is only that of plasticity-induced crack closure. This type of closure is by far the more intensively studied and influential phenomenon for modelling the load interaction effect on FCGR in long cracks. However, in the microstructurally short crack regime, it has been suggested by numerous researchers [6, 21, 25, 26] that plasticity-induced crack closure is not fully developed, which contributes to faster FCGR in short cracks in comparison to that of long cracks. Other types of closure [6, 27], namely oxide-induced and surface roughness-induced closure, which have not been considered in this investigation, are also prevalent in the short crack and the threshold regimes [25]. As a result, users must be extremely cautious in applying the FCGR conversion module to data that are either partially or fully in the short crack regime or near the threshold region.

7. Summary and Future Work

To facilitate the use of the FCGR conversion program DKEFF within DSTO, it was integrated into the CGAP graphical user interface environment. This FCGR conversion program is now known as the FCGR conversion program or module within the CGAP environment. The amalgamation of CGAP and the FCGR conversion module, while significantly enhancing the capability of CGAP as a fatigue crack growth life analysis tool, also provides an easier and more intuitive tool for carrying out the conversion of the nominal FCGR data at multiple stress ratios to a unique da/dN versus ΔK_{eff} curve.

This report presents the theory and the algorithms involved in converting da/dN versus ΔK data to da/dN versus ΔK_{eff} data. It provides an informative source of reference on the use of the CGAP FCGR conversion module. It discusses, in detail, the concept of plasticity-induced crack closure, crack opening stress, the constraint factor α , and the plasticity-corrected SIF. A user manual and examples for the user of this module in CGAP has been presented.

The FCGR conversion module, and more generally CGAP, will continue to be developed and supported by DSTO. Enhancement of the FCGR conversion module will include:

- Providing a means for quantitatively and objectively gauging the quality of the collapsed da/dN versus ΔK_{eff} data;
- Allowing a mixture of CT and CCT specimen data for FCGR conversion;
- The addition of a database capability for da/dN versus ΔK data;
- Implementing a procedure to assist the curve-fitting for the determination of the model parameters in Equation (7), or the visual picking of a list of da/dN versus ΔK_{eff} data, for direct use in CGAP for fatigue crack growth analysis.

Reference

1. Newman, J.C., Jr., FASTRAN II - A fatigue crack growth structural analysis program, NASA TM-104159, 1992.
2. Harter, J.A., AFGROW USERS GUIDE AND TECHNICAL MANUAL, June 2006.
3. Hu, W. and K. Walker. *Fatigue Crack Growth from a Notch under Severe Overload and Underload*. in *The International Conference on Structural Integrity and Failure*. 2006. Sydney, Australia.
4. Hu, W., Y.C. Tong, K.F. Walker, D. Mongru, R. Amaratunga, and P. Jackson, A Review and Assessment of Current Airframe Lining Methodologies and Tools in AVD, DSTO-RR-0321, December 2006.
5. Irwin, G.R., *Analysis of Stresses and Strains near the end of a Crack traversing a plate*. Journal of Applied Physics, 1957: 361.
6. Suresh, S., *Fatigue of Materials*. Cambridge Solid Science Series. 1991, Cambridge: Cambridge University Press.
7. Knott, J.F., *Fundamentals of Fracture Mechanics*. 1973: The Butterworth Group.
8. Suresh, S. and R.O. Ritchie, *Propagation of short fatigue cracks*. International Metals Reviews, 1984. 6: 445.
9. Paris, P.C., M.P. Gomez, and W.E. Anderson, A Rational Analytic Theory of Fatigue.
10. Sharp, P.K., R. Byrnes, and G. Clark, Examination of 7050 Fatigue Crack Growth Data and its Effect on Life Prediction, DSTO-TR-0729, 1998.
11. Elber, W., *Fatigue Crack Closure Under Cyclic Tension*. Engineering Fracture Mechanics, 1970: 37.
12. Elber, W., *The Significance of Fatigue Crack Closure*, in *Damage Tolerance in Aircraft Structures*, A.S.f.T.a. Materials, Editor. 1971: Philadelphia. p. 230.
13. Schijve, J., *Fatigue Crack Closure: Observations and Technical Significance*, in *Mechanics of Fatigue Crack Closure*, J.C.J. Newman and W. Elber, Editors. 1988, American Society for Testing and Materials: Philadelphia. p. 5.
14. Newman, J.C., Jr., *A crack-closure model for predicting fatigue crack growth under aircraft spectrum loading*, in *Methods and Models for Predicting Fatigue Crack Growth under Random Loading*, ASTM STP 748, J.B. Chang and C.M. Hudson, Editors. 1981, ASTM. p. 53.
15. Newman, J.C., Jr. . *Analysis of fatigue crack growth and closure new threshold conditions for large-crack behaviour*. in *ASTM STP-1372*, p. 227. 2000.
16. Newman, J.C.J., FASTRAN-II: A Fatigue Crack Growth Structural Analysis Program, NASA TM 104159.
17. Newman, J.C., Jr., *A crack opening stress equation for fatigue crack growth*. International Journal of Fracture, 1984: R131.
18. SwRI, S.R.I. *A Short Course on DARWIN (Design Assessment of Reliability With Inspection)*. 2003. Melbourne, Australia.
19. Newman, J.C., Jr., *An evaluation of plasticity-induced crack-closure concept and measurement methods*, in *Advances in fatigue crack closure measurement analysis*, ASTM STP 1343, R.C. McClung and J.C.J. Newman, Editors. 1998, American Society for Testing and Materials.

20. Chang, J.B. and J.H. Stolpestad, Improved Methods for Predicting Spectrum Loading Effects-Phase 1 Report, Volume II - Test Data, AFFDL-TR-79-3036, March 1978.
21. Tanaka, K., *Mechanics and Micromechanics of Fatigue Crack Propagation*, in *Fracture Mechanics: Perspective and Directions (Twentieth Symposium)*, ASTM STP 1020, R.P. Wei and R.P. Gangloff, Editors. 1989, American Society for Testing and Materials: Philadelphia. p. 151.
22. Sansoz, F., B. Brethes, and A. Pineau, *Propagation of Short Fatigue Cracks from Notches in a Ni Base Superalloy: Experiments and Modelling*. Fatigue Fracture Engineering Material and Structures, 2001: 41.
23. Newman, J.C.J. *A Non-Linear Fracture Mechanics Approach to the Growth of Small Cracks*. in AGARD Conference Proceedings No. 328, *Behaviour of Short Cracks in Airframe Components*. 1982.
24. Ritchie, R.O. and S. Suresh. *Mechanics of the Growth of Small Cracks*. in AGARD Conference Proceedings No. 328 *Behaviour of Short Cracks in Airframe Components*. 1982.
25. Suresh, S. and R.O. Ritchie, *Propagation of Short Fatigue Cracks*. International Metals Reviews, 1984: 445.
26. Tanaka, K. and Y. Akiniwa, *Mechanics of Small Fatigue Crack Propagation*, in *Small Fatigue Cracks: Mechanics, Mechanisms and Applications*, K.S. Ravichandran, R.O. Ritchie, and Y. Murakami, Editors. 1999, Elsevier Science Ltd. p. 59.
27. Ritchie, R.O., *Mechanisms of Fatigue Crack Propagation in Metals, Ceramics and Composite: Role of Crack Tip Shielding*. Material Science and Engineering, 1988: 15.

Appendix A – CGAP Crack Growth Rate Converter: User Guide

A.1. Introduction

Before running CGAP, FASTRAN or the crack-closure option of AFGROW, it is necessary to convert FCGR versus the nominal SIF range curves at multiple R ratios into a single curve of FCGR versus the effective SIF range. This task is performed in CGAP via the FCGR converter which was developed from the DKEFF program [1]. With the FCGR converter, the user can input the da/dN versus ΔK for different stress ratios, perform the conversion and output elastic or elastic-plastic effective SIF ranges versus da/dN data in graphical and textual format.

This appendix provides information on the use of the FCGR converter in CGAP and includes a flowchart of the basic operations, how to run FCGR, a summary of the major inputs required by FCGR and examples.

A.2. FCGR Program Flowchart

Figure A.1 shows the flowchart of the FCGR program. Included in the flowchart are references to equations in the main body of this report, which are used by FCGR in the determination of the effective SIF.

A.3. Running FCGR

The FCGR module may be run as part of the CGAP software package. Once CGAP has been initiated, go to the *Tools* menu and click on the *Configuration* item. A *Settings* dialog box will appear and the user should then click on the drop down button associated with *Crack-Growth Program Name* to reveal the numerous crack growth CGAP tools. The user should then select the *FCGR Converter* option and click on the *OK* button. This takes the user to the FCGR graphical user interface (GUI). The *Settings* dialog box may also be reached by clicking on the *Configure* icon in the tool bar, see Figure A.2.

The user may then enter the input parameters required to run FCGR via the GUI under the *Geometry*, *Material* and *Case Control* pages or via an input file. For this demonstration, the input file option will be used. The input file may be selected by clicking on the *File* menu item and then selecting the *Import Case* menu item. This will allow the user to select an input file which will load all the necessary parameters required to run the FCGR Converter program. The user should click on the *Yes* button when asked whether they wish to delete the current case. See Figure A.3. The input file must have a *.inp extension. Figure A.4, Figure A.5, and Figure A.6 show the *Geometry*, *Material* and *Case Control* pages respectively after the input file has been loaded. The ΔK versus da/dN data from the input file is automatically plotted (see Figure A.5).

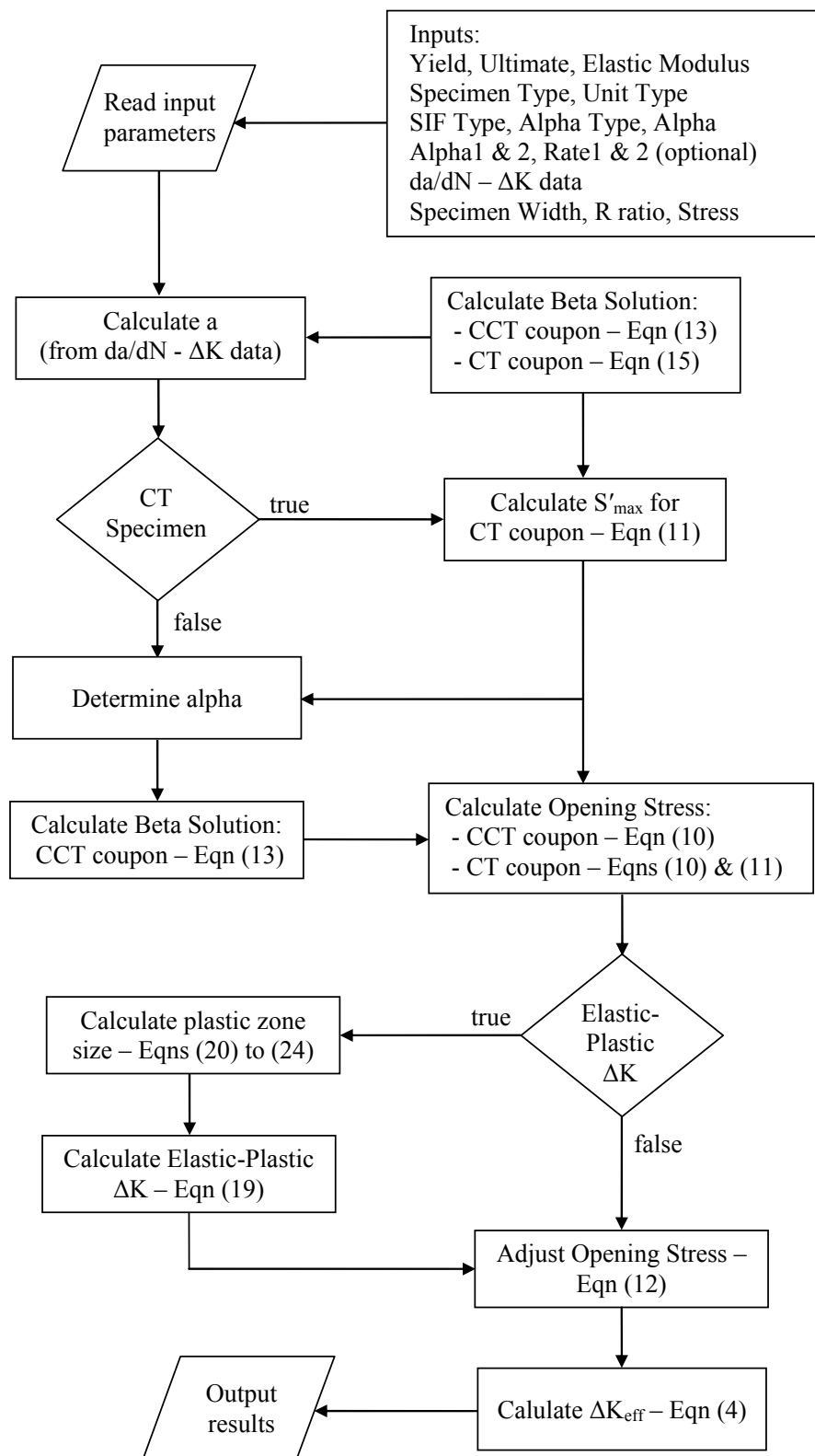


Figure A.1: FCGR Program Flowchart

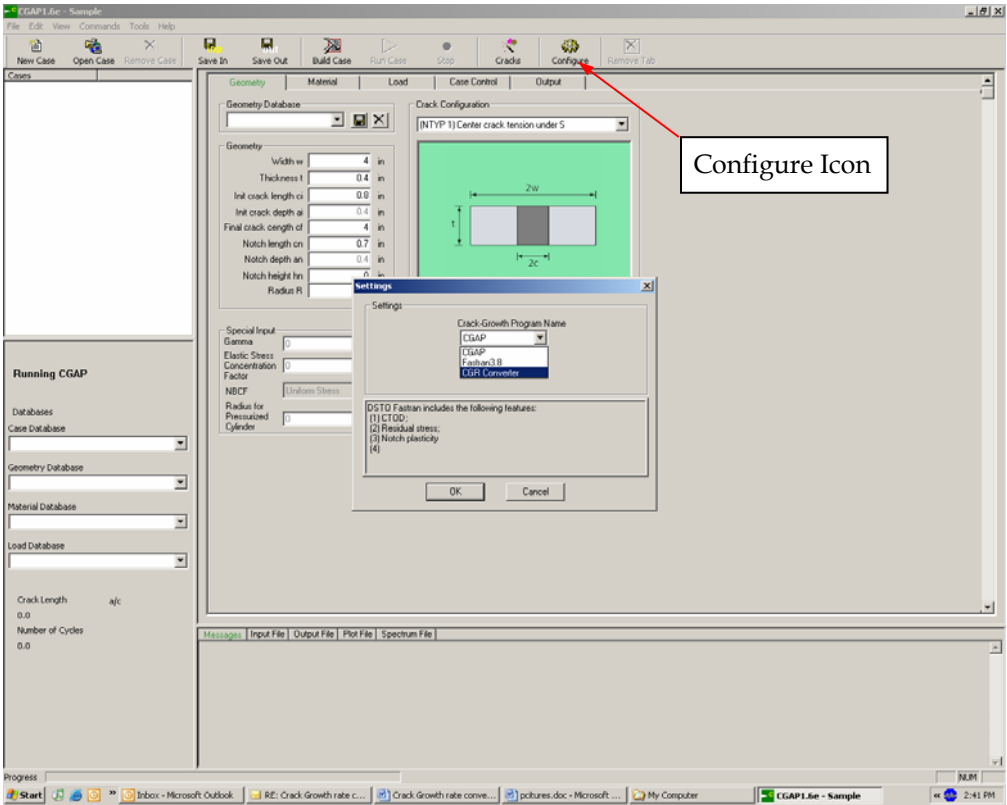


Figure A.2: CGAP Configuration Page

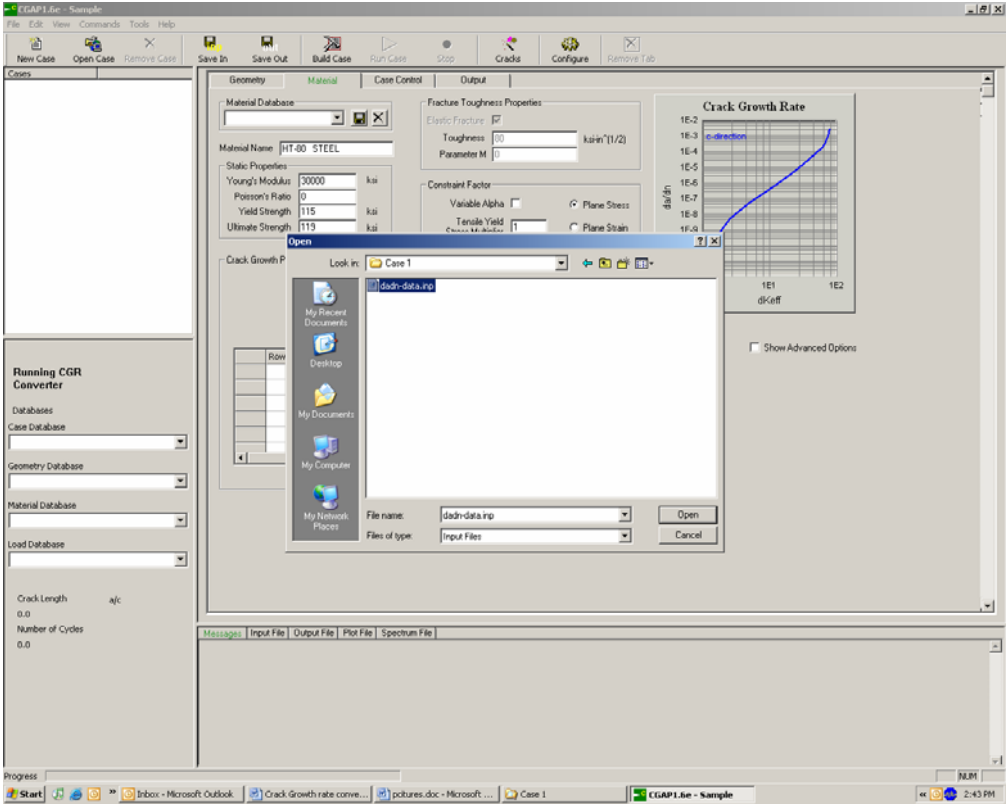


Figure A.3: FCGR Input File Page

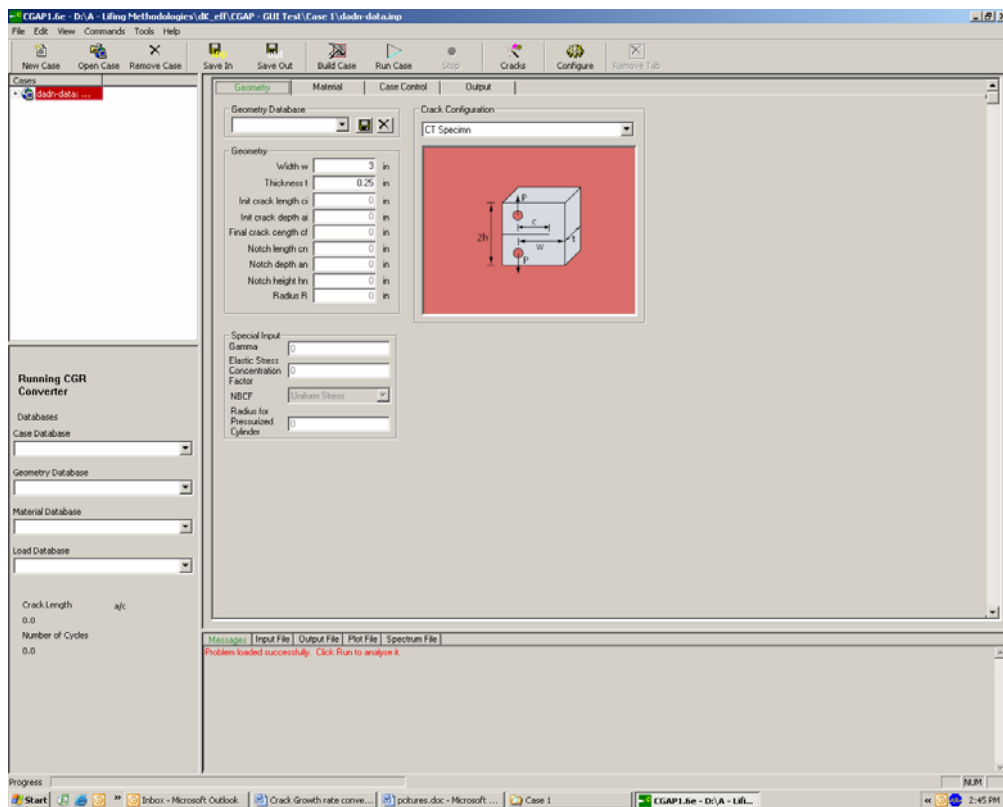


Figure A.4: FCGR Geometry Page

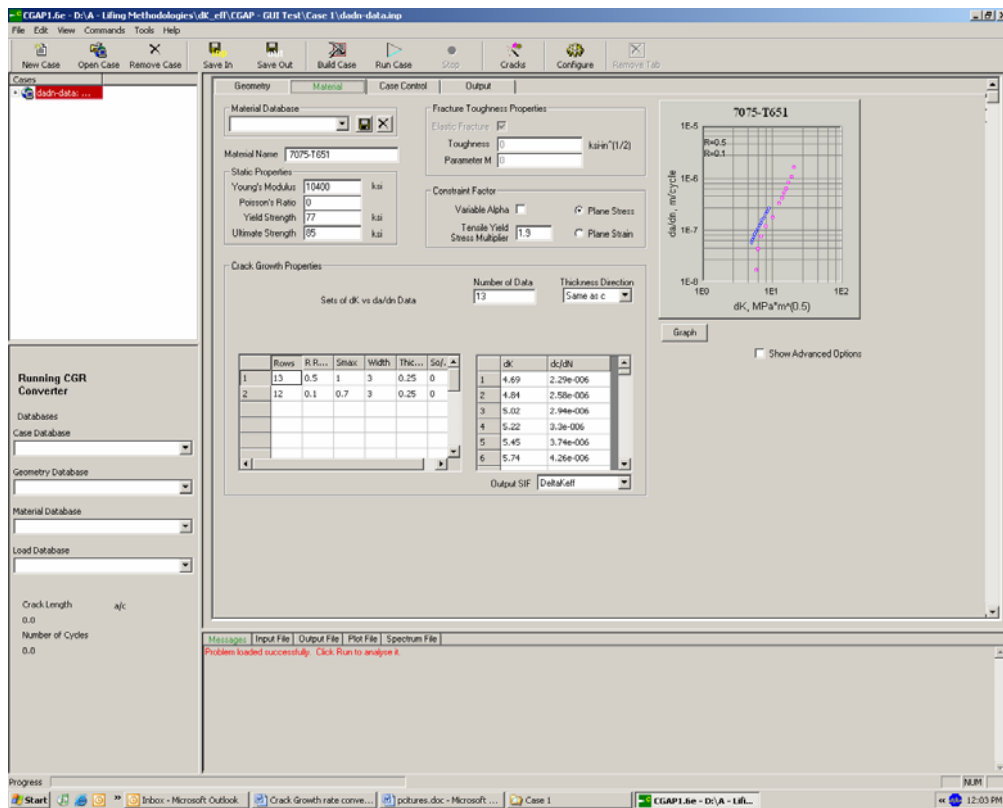


Figure A.5: FCGR Material Page

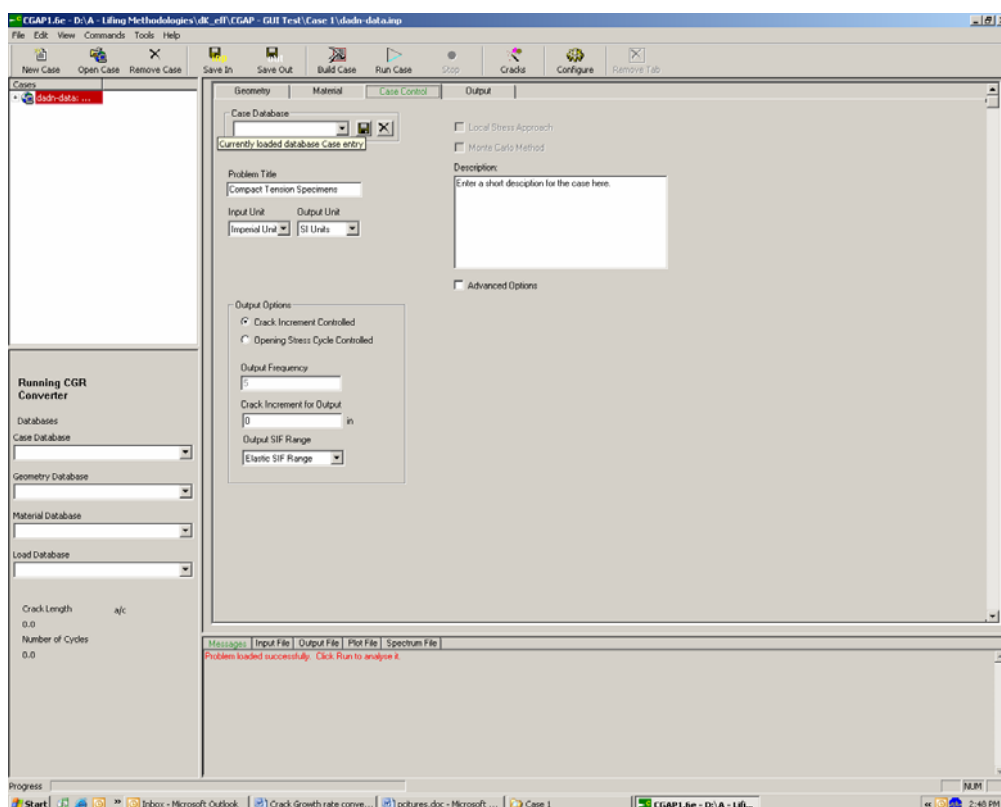


Figure A.6: FCGR Case Control Page

An example input file is shown in Table A.1. A description of the parameters and file format of the input file is provided in Table A.2 and Table A.3. It should be noted that line 5 of the input file (see Table A.2) is optional. If the constraint factor is assumed constant (i.e. $\alpha_{\text{type}} = 0$ in line 4) then line 5 should not appear in the input file. Line 7 contains the da/dN versus ΔK data for a given R ratio and normally contains multiple entries. The combination of lines 6 and 7 may appear multiple times depending on the number of coupon data sets at different R ratios. The example input file of Table A.1 contains 2 coupon data sets at $R = 0.5$ and $R = 0.1$. The S_o/S_{max} parameter in line 7 is optional. Further details regarding its use will be provided in a subsequent paragraph.

Table A.3 includes a reference to the location of each parameter within the FCGR GUI in terms of FCGR page (i.e. *Geometry*, *Material* or *Case Control*) and FCGR page parameter name. This table also describes the options available under each parameter and the parameter value to activate a given option within the input file i.e. if the ΔK versus da/dN data is based on a CT coupon, then Specimen_Type should be set to 2. The FCGR GUI generally uses text in drop down boxes to represent the options. In those instances where the option to select via the GUI is not obvious, the user should refer to Table A.3 and the description of how to run the FCGR tool herein.

To enter or modify the type of elastic-plastic effective SIF calculated by the FCGR tool, first select the *DeltaKbarEff* option from the *Output SIF* drag down box in the *Material* page.

Then tick the *Show Advanced Option* check box in the *Material* page and under the *Effective SIF Modifier* drop down box, select the plastic zone size type. See Table A.3 and Figure A.7.

Figure A.7 also describes the process to manually enter new or edit existing ΔK versus da/dN data.

As described in Section 3, FCGR Converter is unable to calculate crack opening stresses from the input ΔK and stress data if $S_{max}/\sigma_o > 0.6$. In such cases, CGAP or FASTRAN should be used to calculate S_o/S_{max} for each row of ΔK versus da/dN data. The S_o/S_{max} data may then be entered via the input file at line 7 (see Table A.2) or manually under the S_o/S_{max} parameter in the *Material* page. The user must also set Stress_Type to 1 in the input file or S_o/S_{max} to 1 in the *Material* page if the opening stress is determined from CGAP or FASTRAN. Note that Stress_Type (in the input file) or S_o/S_{max} (in the *Material* page) is set to 0 if the opening stress is calculated by FCGR Converter. See Figure A.8.

Table A.1: Example FCGR Input File (dadn-data.inp)

Compact Tension Specimens

7075-T651

2 1

77 85 10400 0 1 1.9 0

2e-005 1.9 0.001 1.2

13 0.5 1 3 0.25

4.69 2.29e-006

4.84 2.58e-006

5.02 2.94e-006

5.22 3.3e-006

5.45 3.74e-006

5.74 4.26e-006

6.07 4.93e-006

6.35 5.5e-006

6.67 6.14e-006

7.08 6.94e-006

7.58 8.17e-006

7.89 9.15e-006

8.26 1.05e-005

12 0.1 0.7 3 0.25

5.43 6.71e-007

5.84 1.72e-006

6.37 3.03e-006

7.41 4.78e-006

9.37 6.82e-006

11.66 1.27e-005

12.79 1.65e-005

13.73 2.07e-005

14.84 2.47e-005

16.02 3.32e-005

17.48 4.16e-005

19.21 6.39e-005

1st coupon data set (at R = 0.5)2nd coupon data set (at R = 0.1)

Table A.2: Input File Format and Parameters

Line	File Parameters
1	Title
2	Material_Name
3	Specimen_Type, Unit_Type
4	Yield, Ultimate, Elastic, SIF_Type, Alpha_Type, Alpha, Stress_Type
5	(Rate1, Alpha1, Rate2, Alpha2 -> optional line)
6	No_Lines, R_Ratio, Stress, Width, Thickness
7	Delta_SIF, da/dN, (So/Smax -> optional parameter)

Table A.3: Detailed Description of FCGR Parameters

Parameter	Description	FCGR Page	FCGR Page Parameter Name
Title	Problem title	Case Control	Problem Title
Material_Name	Name of material	Material	Material Name
Specimen_Type	Specimen type or crack configuration options: = 1 - Centre-crack tension specimen (CCT) = 2 - Compact tension specimen (CT)	Geometry	Crack Configuration
Unit_Type	Type of units options: = 0 - Input and output data have same units = 1 - Input in English units and output in SI units = 2 - Input in SI units and output in English units	Case Control	Input Unit & Output Unit
Yield	Yield strength of material	Material	Static Properties - Yield Strength
Ultimate	Ultimate tensile strength of material	Material	Static Properties - Ultimate Strength
Elastic	Elastic modulus of material	Material	Static Properties - Young's Modulus
SIF_Type	Output SIF options: = 0 - Elastic effective SIF = 1 - Elastic-plastic effective SIF with one-quarter of cyclic plastic zone added to crack length [Eqn (20)] = 2 - Elastic-plastic effective SIF with one-quarter of monotonic plastic zone added to crack length [Eqn (23)] = 3 - Elastic-plastic effective SIF with monotonic plastic zone added to crack length [Eqn (24)]	Material	Crack Growth Properties - Output SIF - For elastic ΔK_{eff} click on <i>DeltaKeff</i> drag down option - For elastic-plastic ΔK_{eff} click on <i>DeltaKbarEff</i> drag down option. Will also need to tick the <i>Show Advanced Option</i> check box and then under the <i>Effective SIF Modifier</i> drag down box, select plastic zone size type.
Alpha_Type	Constraint factor alpha options: = 0 - Constant alpha = 1 - Variable alpha	Material	<i>Constraint Factor - Variable Alpha</i> check box (tick means alpha is variable)
Alpha	Constant constraint factor alpha. Alpha = 1 for the plane-stress condition, 1.73 for Irwin's plane strain and 3 for the plane-strain condition.	Material	Constraint Factor - Tensile Yield Stress Multiplier

Parameter	Description	FCGR Page	FCGR Page Parameter Name
Stress_Type	Calculation of opening stress options: = 0 - FCGR Converter equations = 1 - CGAP/FASTRAN	Material	Crack Growth Properties - So/Smax? Set to 0 if So/Smax is determined by FCGR Converter else set to 1 if CGAP/FASTRAN was used to determine So/Smax.
Rate1	Crack growth rate near start of constraint loss regime (for variable alpha only)	Material	<i>Constraint Factor</i> - Click <i>Edit</i> button once <i>Variable Alpha</i> check box ticked
Alpha1	Alpha at Rate1 (for variable alpha only)	Material	
Rate2	Crack growth rate near end of constraint loss regime (for variable alpha only)	Material	
Alpha2	Alpha at Rate2 (for variable alpha only)	Material	
No_Lines	Number of lines of ΔK versus da/dN data	Material	Crack Growth Properties - Rows
R_Ratio	R ratio (minimum stress/maximum stress) of ΔK versus da/dN specimen data	Material	Crack Growth Properties - R Ratio
Stress	Maximum stress level in constant amplitude specimen test sequence used to generate ΔK versus da/dN data	Material	Crack Growth Properties - Smax
Width	Specimen width	Material*	Crack Growth Properties - Width
Thickness	Specimen thickness	Material*	Crack Growth Properties - Thickness
Delta_SIF	SIF range	Material	Crack Growth Properties - dK
da/dN	Crack growth rate data	Material	Crack Growth Properties - dc/dN
So/Smax	Ratio of the opening stress to the maximum stress determined from CGAP or FASTRAN	Material	Crack Growth Properties - So/Smax

* Also found in the *Geometry* page. However, value at *Material* page overrides *Geometry* page entry.

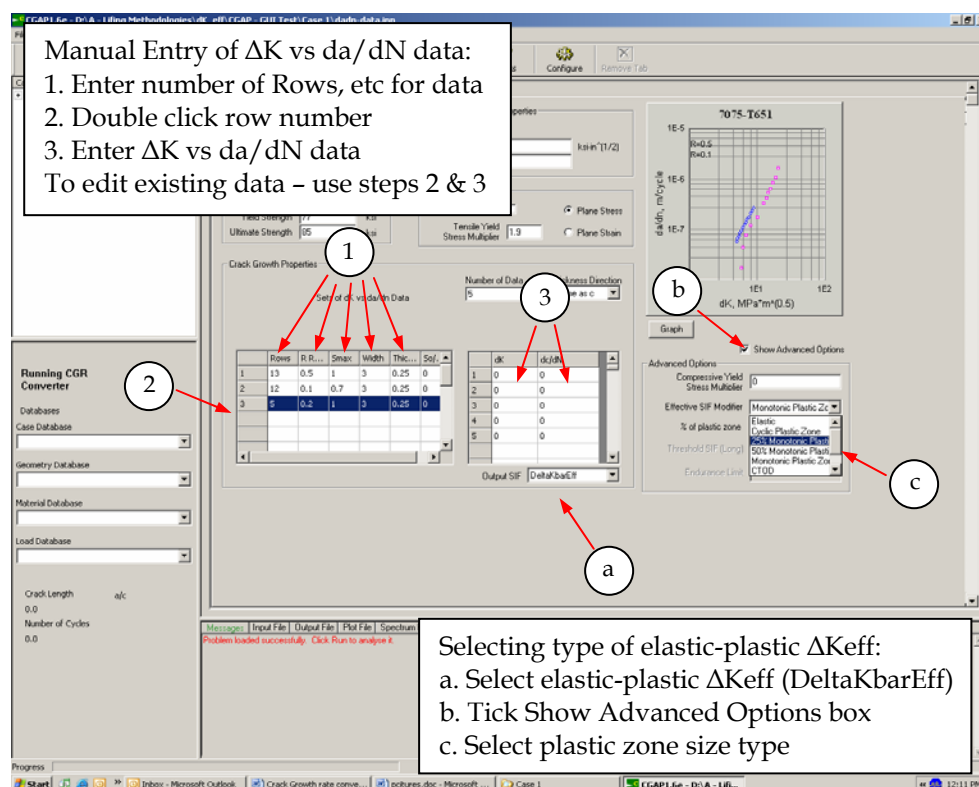


Figure A.7: Entering Crack Growth Data and Selecting Type of Effective SIF

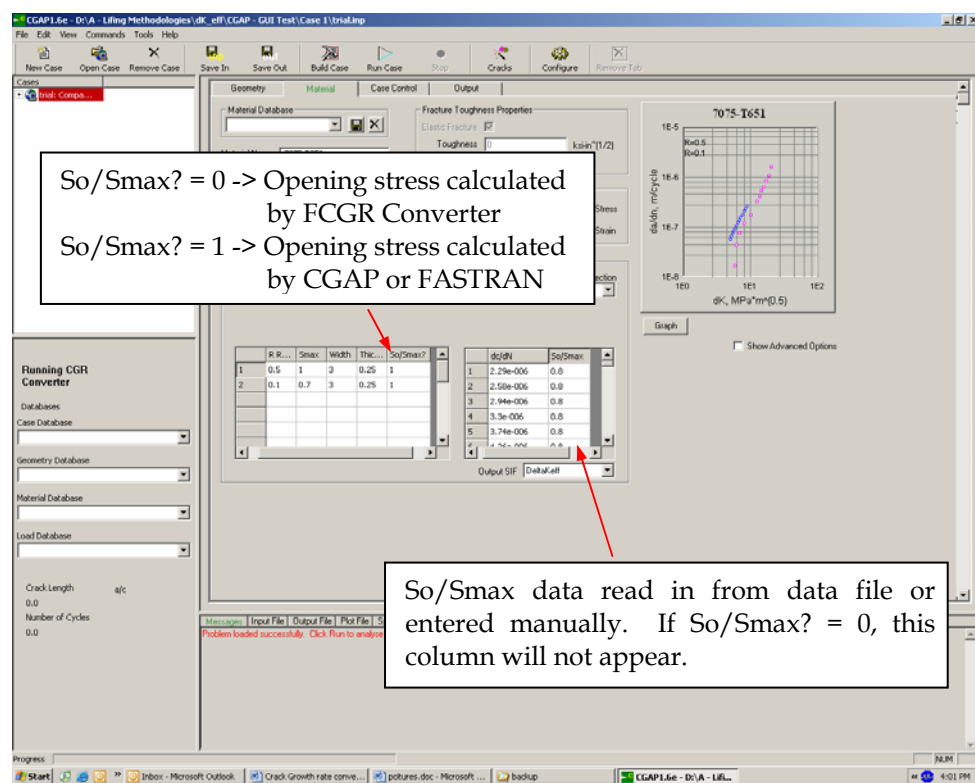


Figure A.8: Location of So/Smax Data within Material Page

Once the input parameters have been set, it is necessary to specify the type of output the user desires. In the *Case Control* page under *Output Options*, the FCGR parameter *Output SIF Range* may be used to output either, elastic or effective SIF ranges. See Figure A.9.

The user then builds the case by clicking on the build button and finally runs the case by clicking on the run button (see Figure A.9). Alternatively, the *Build* and *Run* commands may be accessed via the *Commands* menu.

Upon successful execution of the FCGR program the results may be viewed via the GUI by clicking on the *Graph* button in the *Material* page (see Figure A.10). This may be useful for quickly evaluating the effect of different alpha values as the user can change the alpha value(s), build/run the case and then hit the *Graph* button to get immediate feedback on the impact of the change. Existing or updated parameter values may also be saved to an input file by going to the *File* menu and clicking on the *Export Case* item.

After running the program, two output files will have been created; one with a *.out extension and the other with a *.plt extension. The output file basename (i.e. that part of the filename before the ".") will be the same as the input file's basename. An example *.out file is shown in Table A.4. This file contains the R ratio and stress level for each coupon data set as well as the effective ΔK , da/dN , the ratio of the opening stress to the maximum stress, the maximum stress, the constraint factor and the crack length for each row of ΔK versus da/dN data within the input file. An example *.plt file is shown in Table A.5 It contains almost the same information as the *.out file but in a slightly different format which may be more useful for plotting in Excel. The input and output files as well as program messages may be reviewed within the FCGR tool by clicking on the toolbar highlighted in Figure A.10.

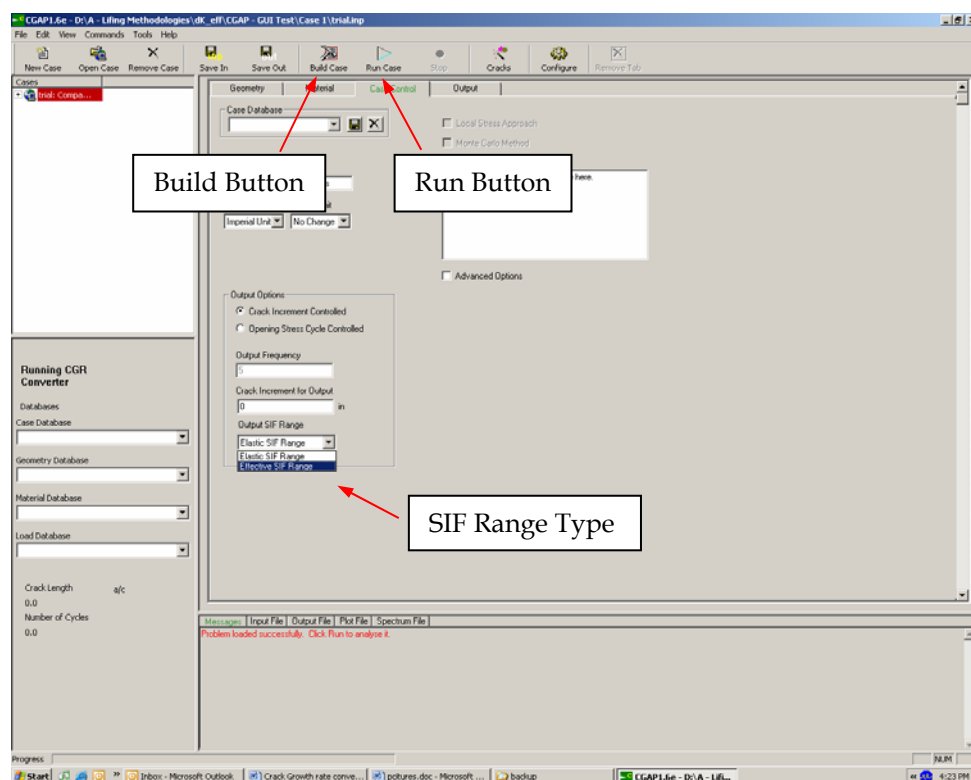


Figure A.9: Select Type of SIF Range and Run Problem

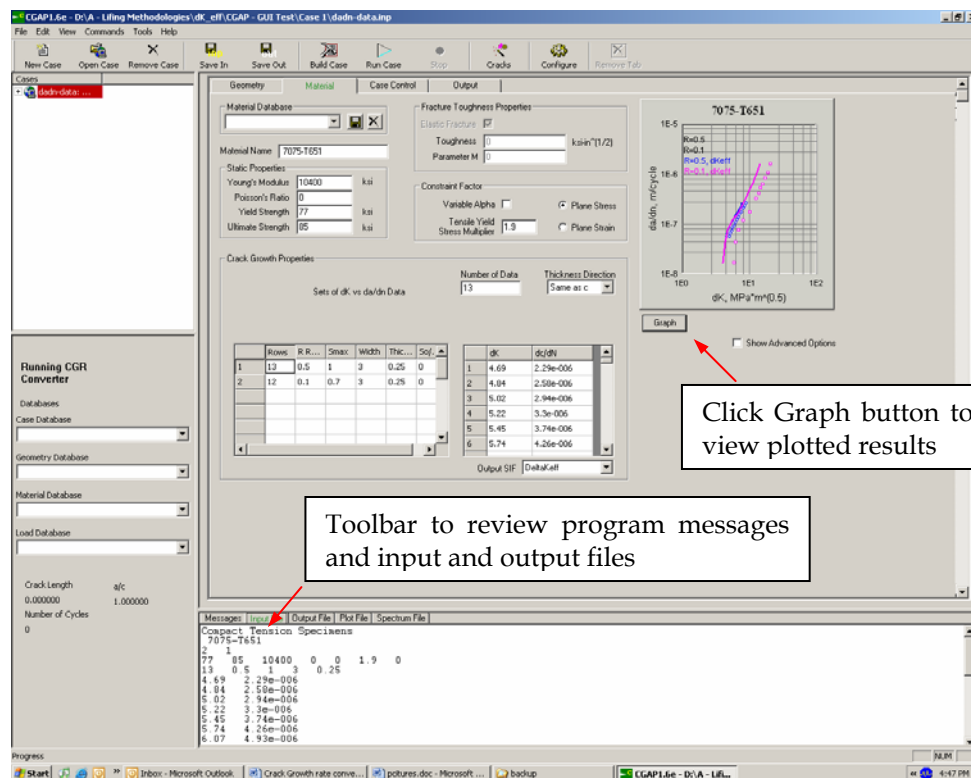


Figure A.10: FCGR Graph Function and Input/Output File Review

Table A.4: Sample *.out Output File

DKEFF ELASTIC R = 0.50 Smax = 6.89 MPa

DKEFF	RATE	So/Smax`	Smax`	ALP	c
MPa-m ^{0.5}	m/cycle		MPa	m	
0.4500E+01	0.5817E-07	0.5635E+00	0.3741E+02	0.1900E+01	0.2177E-01
0.4641E+01	0.6553E-07	0.5637E+00	0.3764E+02	0.1900E+01	0.2269E-01
0.4811E+01	0.7468E-07	0.5639E+00	0.3793E+02	0.1900E+01	0.2377E-01
0.5001E+01	0.8382E-07	0.5641E+00	0.3826E+02	0.1900E+01	0.2493E-01
0.5220E+01	0.9500E-07	0.5643E+00	0.3866E+02	0.1900E+01	0.2621E-01
0.5496E+01	0.1082E-06	0.5644E+00	0.3918E+02	0.1900E+01	0.2775E-01
0.5810E+01	0.1252E-06	0.5645E+00	0.3981E+02	0.1900E+01	0.2939E-01
0.6077E+01	0.1397E-06	0.5646E+00	0.4036E+02	0.1900E+01	0.3069E-01
0.6382E+01	0.1560E-06	0.5647E+00	0.4101E+02	0.1900E+01	0.3209E-01
0.6774E+01	0.1763E-06	0.5647E+00	0.4187E+02	0.1900E+01	0.3375E-01
0.7250E+01	0.2075E-06	0.5649E+00	0.4295E+02	0.1900E+01	0.3558E-01
0.7543E+01	0.2324E-06	0.5650E+00	0.4363E+02	0.1900E+01	0.3663E-01
0.7893E+01	0.2667E-06	0.5652E+00	0.4445E+02	0.1900E+01	0.3779E-01

DKEFF ELASTIC R = 0.10 Smax = 4.83 MPa

DKEFF	RATE	So/Smax`	Smax`	ALP	c
MPa-m ^{0.5}	m/cycle		MPa	m	
0.4145E+01	0.1704E-07	0.3748E+00	0.2582E+02	0.1900E+01	0.1935E-01
0.4438E+01	0.4369E-07	0.3777E+00	0.2613E+02	0.1900E+01	0.2143E-01
0.4826E+01	0.7696E-07	0.3796E+00	0.2659E+02	0.1900E+01	0.2398E-01
0.5606E+01	0.1214E-06	0.3804E+00	0.2761E+02	0.1900E+01	0.2846E-01
0.7096E+01	0.1732E-06	0.3798E+00	0.2984E+02	0.1900E+01	0.3508E-01
0.8816E+01	0.3226E-06	0.3808E+00	0.3269E+02	0.1900E+01	0.4052E-01
0.9663E+01	0.4191E-06	0.3813E+00	0.3412E+02	0.1900E+01	0.4259E-01
0.1035E+02	0.5258E-06	0.3827E+00	0.3532E+02	0.1894E+01	0.4409E-01
0.1110E+02	0.6274E-06	0.3875E+00	0.3673E+02	0.1862E+01	0.4564E-01
0.1181E+02	0.8433E-06	0.3964E+00	0.3821E+02	0.1809E+01	0.4710E-01
0.1274E+02	0.1057E-05	0.4030E+00	0.4003E+02	0.1769E+01	0.4866E-01
0.1367E+02	0.1623E-05	0.4172E+00	0.4215E+02	0.1692E+01	0.5025E-01

Table A.5: Sample *.plt Plot File

Compact Tension Specimens

13 0.50

0.4500E+01	0.5817E-07	0.5635E+00	0.3741E+02	0.1900E+01	0.2177E-01
0.4641E+01	0.6553E-07	0.5637E+00	0.3764E+02	0.1900E+01	0.2269E-01
0.4811E+01	0.7468E-07	0.5639E+00	0.3793E+02	0.1900E+01	0.2377E-01
0.5001E+01	0.8382E-07	0.5641E+00	0.3826E+02	0.1900E+01	0.2493E-01
0.5220E+01	0.9500E-07	0.5643E+00	0.3866E+02	0.1900E+01	0.2621E-01
0.5496E+01	0.1082E-06	0.5644E+00	0.3918E+02	0.1900E+01	0.2775E-01
0.5810E+01	0.1252E-06	0.5645E+00	0.3981E+02	0.1900E+01	0.2939E-01
0.6077E+01	0.1397E-06	0.5646E+00	0.4036E+02	0.1900E+01	0.3069E-01
0.6382E+01	0.1560E-06	0.5647E+00	0.4101E+02	0.1900E+01	0.3209E-01
0.6774E+01	0.1763E-06	0.5647E+00	0.4187E+02	0.1900E+01	0.3375E-01
0.7250E+01	0.2075E-06	0.5649E+00	0.4295E+02	0.1900E+01	0.3558E-01
0.7543E+01	0.2324E-06	0.5650E+00	0.4363E+02	0.1900E+01	0.3663E-01
0.7893E+01	0.2667E-06	0.5652E+00	0.4445E+02	0.1900E+01	0.3779E-01

Compact Tension Specimens

12 0.10

0.4145E+01	0.1704E-07	0.3748E+00	0.2582E+02	0.1900E+01	0.1935E-01
0.4438E+01	0.4369E-07	0.3777E+00	0.2613E+02	0.1900E+01	0.2143E-01
0.4826E+01	0.7696E-07	0.3796E+00	0.2659E+02	0.1900E+01	0.2398E-01
0.5606E+01	0.1214E-06	0.3804E+00	0.2761E+02	0.1900E+01	0.2846E-01
0.7096E+01	0.1732E-06	0.3798E+00	0.2984E+02	0.1900E+01	0.3508E-01
0.8816E+01	0.3226E-06	0.3808E+00	0.3269E+02	0.1900E+01	0.4052E-01
0.9663E+01	0.4191E-06	0.3813E+00	0.3412E+02	0.1900E+01	0.4259E-01
0.1035E+02	0.5258E-06	0.3827E+00	0.3532E+02	0.1894E+01	0.4409E-01
0.1110E+02	0.6274E-06	0.3875E+00	0.3673E+02	0.1862E+01	0.4564E-01
0.1181E+02	0.8433E-06	0.3964E+00	0.3821E+02	0.1809E+01	0.4710E-01
0.1274E+02	0.1057E-05	0.4030E+00	0.4003E+02	0.1769E+01	0.4866E-01
0.1367E+02	0.1623E-05	0.4172E+00	0.4215E+02	0.1692E+01	0.5025E-01

A.4. Example Problem Using 7075-T651

An example of the conversion of da/dN versus ΔK data into effective da/dN versus ΔK_{eff} data is provided in this section. The problem will use the information provided in Section A.3 for aluminium 7075-T651. The da/dN versus ΔK were obtained from [16] from $R = 0.5$ and $R = 0.1$ constant amplitude tests on compact tension specimens. The data are shown in the FCGR input file format in Table A.1. The problem utilises variable constraint factors/rates which are provided in the input file (line 5 in Table A.1). These values were determined by Newman through trial and error until the two ΔK versus da/dN data sets collapsed into a single set of effective ΔK versus da/dN data. The input file of Table A.1 was run through the FCGR program and the two files shown in Table A.4 and Table A.5 were output. These files contain the elastic effective ΔK versus da/dN data which is plotted in Figure A.11. As can be seen in Figure A.11, the constraint factors selected by Newman have successfully collapsed the two ΔK versus da/dN data sets into a single elastic effective ΔK versus da/dN curve.

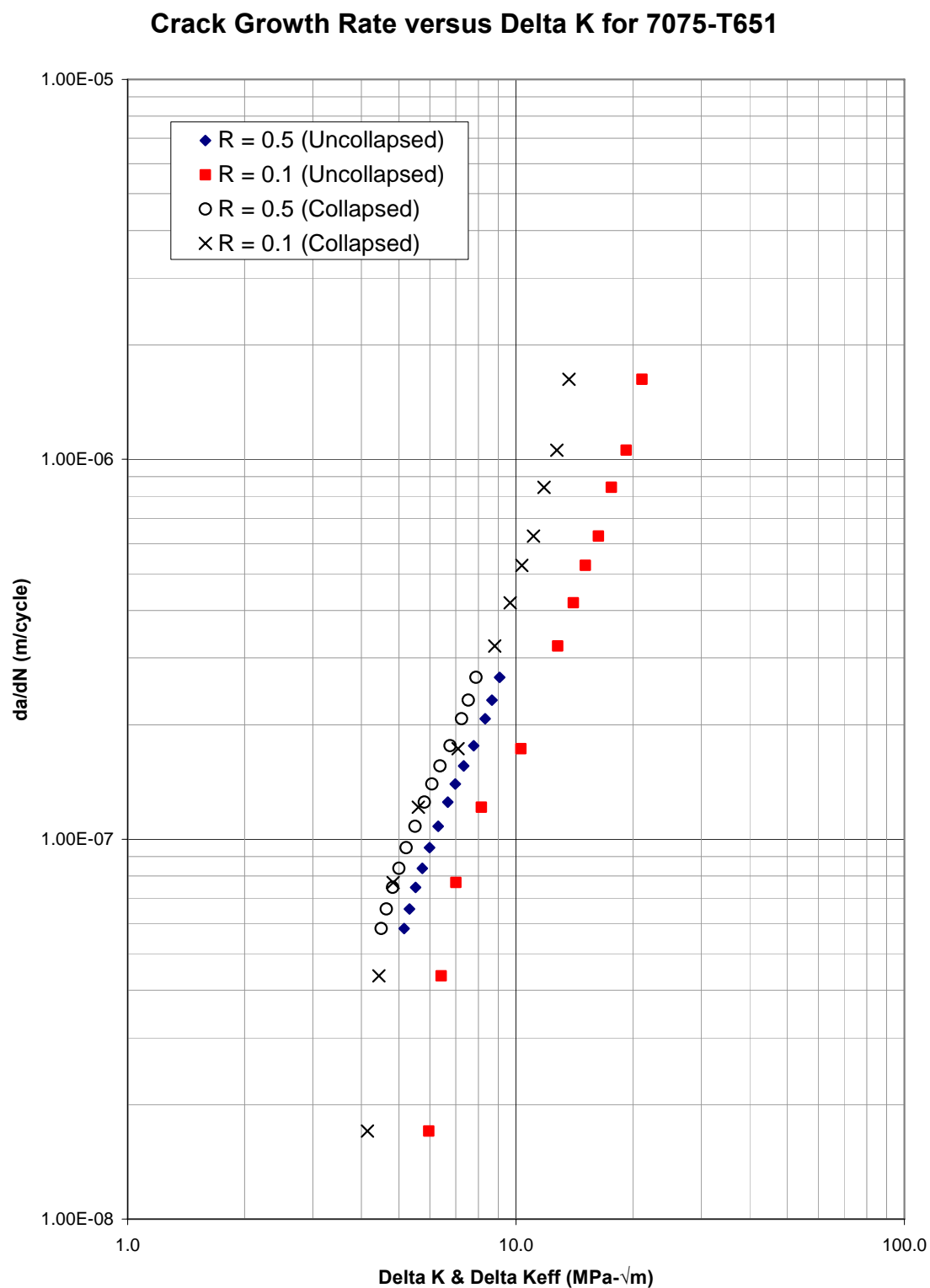


Figure A.11: da/dN versus ΔK for 7075-T651

Appendix B - Coefficient of Determination

The coefficient of determination, commonly denoted as R^2 , can be employed to provide a means for quantitatively measuring how well a regression fits to the observed data. It is given as,

$$R^2 = 1 - \frac{\sum_{i=1}^I (f(x) - y)^2}{\sum_{i=1}^I y^2 - \frac{\left(\sum_{i=1}^I y\right)^2}{I}}$$

where generally, $f(x)$ is the predicted value as a function of the variable x , y is the observed value, and I is the total number of observations. The coefficient of determination is such that $0 \leq R^2 \leq 1$. $R^2 = 1$ if the regression provides a perfect fit through every observation point, and $R^2 = 0$ if the observed data is completely independent of x . Based on this method, the optimum α is obtained by finding the maximum value of R^2 .

Appendix C Input Files for the Examples

The input files for the examples are now part of the CGAP distribution. Once CGAP is installed, these files, together with the corresponding output files (*.out) and the plot files (*.plt), reside in the following directory, e.g.,

C:\Programs Files\DSTO\CGAP\Samples\FCGR

The file names for the examples are given as below.

Section	Example	Input File Name
5.1.2 (p. 22)	7050-T7451, variable constraint	7050T7451_variable_alpha.inp
5.2.2 (p. 25)	2219-T851, variable constraint	2219T851_variable_alpha_1.inp
5.2.2 (p. 25)	2219-T851, variable constraint	2219T851_variable_alpha_2.inp

DEFENCE SCIENCE AND TECHNOLOGY ORGANISATION DOCUMENT CONTROL DATA					
				1. PRIVACY MARKING/CAVEAT (OF DOCUMENT)	
2. TITLE A Crack Growth Rate Conversion Module: Theory, Development, User Guide and Examples			3. SECURITY CLASSIFICATION (FOR UNCLASSIFIED REPORTS THAT ARE LIMITED RELEASE USE (L) NEXT TO DOCUMENT CLASSIFICATION) Document (U) Title (U) Abstract (U)		
4. AUTHOR(S) Yu Chee Tong, Weiping Hu and David Mongru			5. CORPORATE AUTHOR DSTO Defence Science and Technology Organisation 506 Lorimer St Fishermans Bend Victoria 3207 Australia		
6a. DSTO NUMBER DSTO-TR-2050		6b. AR NUMBER AR-014-020		7. DOCUMENT DATE September 2007	
8. FILE NUMBER 2007/1071051/1		9. TASK NUMBER AIR 06/151		10. TASK SPONSOR DGTA-ASI	
				11. NO. OF PAGES 48	
				12. NO. OF REFERENCES 28	
13. URL on the World Wide Web http://www.dsto.defence.gov.au/corporate/reports/DSTO-TR-2050.pdf			14. RELEASE AUTHORITY Chief, Air Vehicles Division		
15. SECONDARY RELEASE STATEMENT OF THIS DOCUMENT <p style="text-align: center;"><i>Approved for public release</i></p>					
OVERSEAS ENQUIRIES OUTSIDE STATED LIMITATIONS SHOULD BE REFERRED THROUGH DOCUMENT EXCHANGE, PO BOX 1500, EDINBURGH, SA 5111					
16. DELIBERATE ANNOUNCEMENT No Limitations					
17. CITATION IN OTHER DOCUMENTS Yes					
18. DSTO RESEARCH LIBRARY THESAURUS http://web-vic.dsto.defence.gov.au/workareas/library/resources/dsto_thesaurus.htm crack growth rate, crack closure model, fatigue crack					
19. ABSTRACT The use of crack growth analysis tools based on plasticity-induced crack closure model, such as FASTRAN, CGAP and AFGROW, requires the conversion of crack growth rate versus the nominal stress intensity range curves to a "single" curve of crack growth rate versus the effective stress intensity range. In order to minimise the error arising from crack growth rate conversion and judiciously utilise these software tools, a user-friendly tool integrated into CGAP. This report documents the theory, implementation, the user guide and examples of the crack growth rate conversion software module.					